Polyhedron 243 (2023) 116565

Contents lists available at ScienceDirect

Polyhedron

journal homepage: www.elsevier.com/locate/poly

Three-coordinate monoanions of rhodium(1–) and iridium(1–): Isolable examples of coordinatively-unsaturated metalate anions

Michael L. Neville, Chinglin Chan, Brandon R. Barnett, Ritchie E. Hernandez, Curtis E. Moore, Joshua S. Figueroa *

Department of Chemistry and Biochemistry, University of California, San Diego, 9500 Gilman Drive, MC 0358, La Jolla, CA 92093, USA

ARTICLE INFO

Keywords:
Metalates
Nucleophiles
Lewis-acid interactions
Rhodium
Iridium

ABSTRACT

Metalate complexes – those that possess metal centers in formally negative oxidation states – are typically coordinatively and electronically saturated organometallic species. The reduced nature of the metal centers within these complexes is well understood to be responsible for their high reactivity as metal-based nucleophiles. While the chemistry of such complexes is extensive, there are very few examples where coordinative or electronic unsaturation accompanies highly-reduced d-orbital manifolds as a means to augment reactivity. Reported here is the isolation of the 16e$^-$, d^{10} rhodium and iridium metalate anions, [M(CNAr^{Dipp2})$_3$]$^-$, where coordinative unsaturation is achieved through the use of encumbering *m*-terphenyl isocyanide ligands. Reactivity studies with electrophiles demonstrate that the Rh and Ir centers in these metalates retain significant nucleophilic character, which enables the formation of unusual metal/main-group-element species on account of low coordination numbers.

1. Introduction

Organometallic complexes with metal centers in formally negative oxidation states have enjoyed a rich history due to their high reactivity and unique electronic structure properties [1–7]. In order to stabilize the highly reduced metal centers in these so-called metalates, it has long been recognized that π-acidic ligands provide the most straight-forward route to delocalize excess electron density away from the metal center. Accordingly, metalates featuring π -acidic ligands such as CO, isocyanides (CNR), olefins, arenes and PF_3 have been reported for a wide range of transition metals [3,4,7]. However, a commonality shared by the overwhelming majority of metalates is that their metal centers possess coordinative or electronic saturation [4]. This feature has arisen from both the small steric profile of the ligands employed for isolation of metalate complexes, and the stability gained from delocalizing excess electron density over as many π -acidic ligands as possible. While some metalate complexes, particularly those championed by Ellis, feature low coordination numbers [8–10], electronic saturation in the form of formal addition of electrons to vacant coordination sites imparts stability to these complexes by allowing the metal center to reach an 18e$^-$ configuration [3,4]. Indeed, very few mononuclear metalate complexes have been isolated that feature metal centers with an electron count less than seventeen [4,7,11–13]. This is despite the fact that imparting a degree of coordinative unsaturation to otherwise highly-reducing and nucleophilic metal centers could significantly enhance their reactivity properties.

A reasonable strategy for the preparation of coordinatively-unsaturated metalate complexes is the employment of sterically encumbering π -acidic ligands. Our group has previously investigated this approach using the *m*-terphenyl isocyanide ligand CNAr^{Mes2} (Ar^{Mes2} = 2,6-(2,4,6-Me$_3$C$_6$H$_2$)$_2$C$_6$H$_3$) [14], which features two flanking mesityl substituents. While several monomeric isocyanometalates of Mn, Fe and Co have been prepared with CNAr^{Mes2} [15–20], each has featured coordinative saturation and an 18e$^-$ configuration. We therefore sought to define a metalate system that was inherently coordinatively unsaturated, such that substrate binding and activation events could be unimpeded. Herein we report the actualization of this goal and the synthesis of the 16e$^-$, Group 9 metalate monanions [Rh(CNAr^{Dipp2})$_3$]$^-$ and [Ir(CNAr^{Dipp2})$_3$]$^-$, where the CNAr^{Dipp2} ligand is a more sterically encumbering *m*-terphenyl isocyanide derivative (Ar^{Dipp2} = 2,6-(2,6-(*i*-Pr)$_2$C$_6$H$_3$)$_2$C$_6$H$_3$) [21–23]. Both [Rh(CNAr^{Dipp2})$_3$]$^-$ and [Ir(CNAr^{Dipp2})$_3$]$^-$ display electronic-structure characteristics consistent with their low coordination number, but react as effective metal-based nucleophiles. In addition, we compare and contrast the reactivity

* Corresponding author.
E-mail address: jsfig@ucsd.edu (J.S. Figueroa).

https://doi.org/10.1016/j.poly.2023.116565
Received 13 January 2023; Accepted 15 July 2023
Available online 20 July 2023

properties of these Rh and Ir metalates with that of the cobalt derivative, $[Co(CNAr^{Dipp2})_3]^-$, and uncover an unusual situation where the heavier Group 9 complexes display weaker Lewis-acidity properties than their lighter congener.

2. Results and discussion

Synthetic entry to three-coordinate Rh and Ir metalates was provided by the monovalent d^8 complexes, $MCl(CNAr^{Dipp2})_3$ (M = Rh (**1**), Ir (**2**)), which were obtained via the reaction between the dimers, $[MCl(COD)]_2$ (M = Rh, Ir; COD = 1,5-cyclooctadiene), with 6.0 equiv of $CNAr^{Dipp2}$. The ^1H NMR spectra of complexes **1** and **2** both featured a 2:1 ratio of Ar^{Dipp2} residues, which is diagnostic of a square planar coordination geometry. This was confirmed by crystallographic analysis (Figs. S2.1 and S2.2) and it is important to note that the IR spectra of complexes **1** and **2** each possess three ν_{CN} bands in the range of 2156–1967 cm^{-1}, consistent with both a C_{2v}-symmetric coordination environment and moderate π-backdonation to the $CNAr^{Dipp2}$ ligand π* orbitals (ν_{CN} for free $CNAr^{Dipp2}$ = 2118 cm^{-1}) [21].

Treatment of bright yellow complexes **1** or **2** with potassium graphite (KC_8) in cold Et_2O solution resulted in the formation of dark red solutions over the course of 1 h (Scheme 1). For both reactions, analysis by ^1H NMR spectroscopy revealed the formation of one new product, each possessing a single $CNAr^{Dipp2}$ ligand environment. The IR spectra of these reduction products revealed a series of broad overlapping ν_{CN} bands in the region between 2100 cm^{-1} to 1800 cm^{-1}. Relative to complexes **1** and **2**, these shifts to lower energy indicate the presence of more reduced metal centers, while broadness of the bands are consistent with other isocyanometalates that form tight ion-pairing interactions between the isocyanide C≡N units and alkali metal cations [15,16,18,24]. Structural determination on crystals grown from Et_2O solution under an N_2 atmosphere identified these products as the three-coordinate metalate salts $K[Rh(CNAr^{Dipp2})_3]$ (K[**3**]) and $K[Ir(CNAr^{Dipp2})_3]$ (K[**4**]), which are indeed unsolvated, contact ion-pairs in the solid state (Fig. 1) [25,26]. The Rh and Ir centers in K[**3**] and K[**4**], respectively, adopt planar coordination environments, as has been predicted for the unstable, gas-phase 16e⁻ carbonylmetalate species $[Rh(CO)_3]^-$ and $[Ir(CO)_3]^-$ to which they are most analogous [27]. In addition, complexes K[**3**] and K[**4**] give rise to significantly downfield $^{13}C\{^1H\}$ NMR chemical shifts of 212.9 ppm and 225.5 ppm, respectively, for their isocyanide carbon atoms. Such downfield chemical shifts are markers of significant π-backbonding to isocyanide ligands and reflect the presence of highly reduced metal centers [18,28–30], despite the coincidence of a formally 16e⁻, coordinatively-unsaturated primary coordination sphere.

While the metal centers in K[**3**] and K[**4**] adopt three-coordinate environments, inspection of their solid-state structures reveal a distortion from an idealized trigonal planar coordination geometry. This is illustrated by the contracted C1-M−C2 angles of 113.0(13)° and 112.11(17)° for complexes K[**3**] and K[**4**], respectively, on account of the cation-π(CN) contacts. Accordingly, in an effort to evaluate the structural features of these three-coordinate metalates in the absence of ion pairing, cation encapsulation studies were conducted with [2.2.2]-cryptand. Salts K[**3**] and K[**4**] both reacted readily with [2.2.2]-cryptand in THF solution to form the separated ion pairs [K(crypt)][**3**] and [K(crypt)][**4**] as determined by X-ray crystallography (Scheme 1; Fig. 1). Most remarkably, the $[M(CNAr^{Dipp2})_3]^-$ anions in [K(crypt)][3] and [K(crypt)][4] also deviate from an idealized D_{3h}-symmetric coordination geometry. Instead, they adopt pronounced C_{2v}-symmetric, Y-shaped structures on account of expanded C2-M−C3 bond angles (125.7(2)° and 126.9(8)° for [K(crypt)][**3**] and [K(crypt)][**4**], respectively).

It is important to note that this Y-shaped structural feature is retained in solution and represents a distinct electronic interplay between σ- and π-ligand field effects. For example, the solution-phase IR spectra (C_6D_6) of [K(crypt)][**3**] and [K(crypt)][**4**] both give rise to three well-separated ν_{CN} bands. This pattern indicates that C_{2v}-symmetric geometries for the Rh and Ir centers are retained in solution, despite the fact that ion-pairing contacts have been removed by the presence of the cryptand. Notably, DFT calculations (B3LYP/LANL2DZ) on the truncated model complex $[Rh(CNAr^{Ph2})_3]^-$ reveal the origin of this structural effect. As shown in Fig. 2, the calculated HOMO for $[Rh(CNAr^{Ph2})_3]^-$ is of distinct $d(x^2\text{-}y^2)$ parentage. This contrasts with the related 16e⁻ d^{10} nickel triisocyanide complex, $Ni(CNAr^{Dipp2})_3$ [31], for which the dz^2 orbital is the calculated HOMO on account of a near perfect D_{3h}-symmetric coordination geometry [32]. Indeed, in D_{3h}-symmetry, both the e'($x^2\text{-}y^2$, xy) and e''(xz,yz) orbital sets are expected to be energetically stabilized by the two orthogonal π* orbital sets of the isocyanide ligands, thereby rendering the a_1'-symmetric dz^2 orbital highest-lying. For $[Rh(CNAr^{Ph2})_3]^-$, the good σ-donating character of the isocyanide ligands [19], coupled with the greater radial extension of the 4d orbitals, combine to create a strong ligand field in the σ-bonding direction. This effect is well recognized for square-planar d^8 complexes of late 4d and

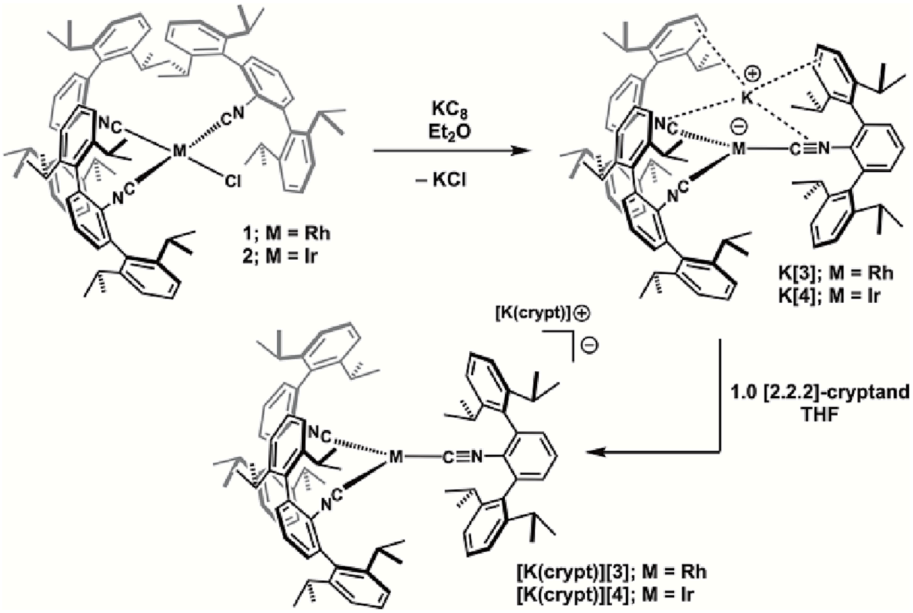

Scheme 1. Synthesis of three-coordinate Rh and Ir metalate anions.

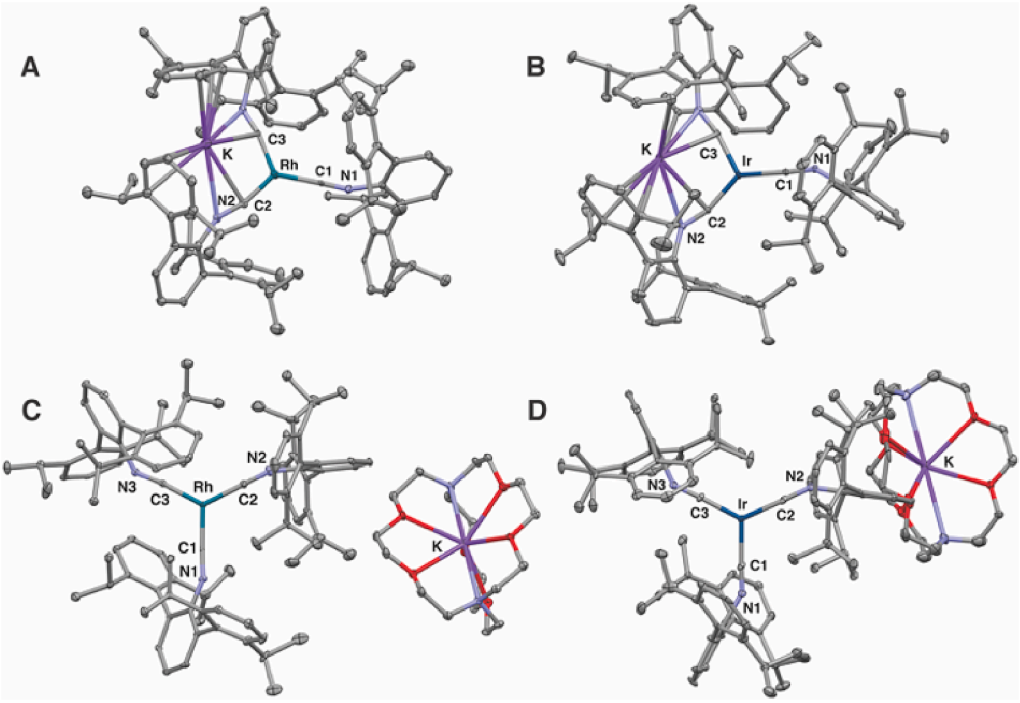

Fig. 1. Molecular structures of (A) K[Rh(CNAr^{Dipp2})$_3$] (K[**3**]), (B) K[Ir(CNAr^{Dipp2})$_3$] (K[**4**]), (C) [K([2.2.2]-cryptand)][Rh(CNAr^{Dipp2})$_3$] ([K(crypt)][**3**]) and (D) [K([2.2.2]-cryptand)][Ir(CNAr^{Dipp2})$_3$] ([K(crypt)][**4**]).

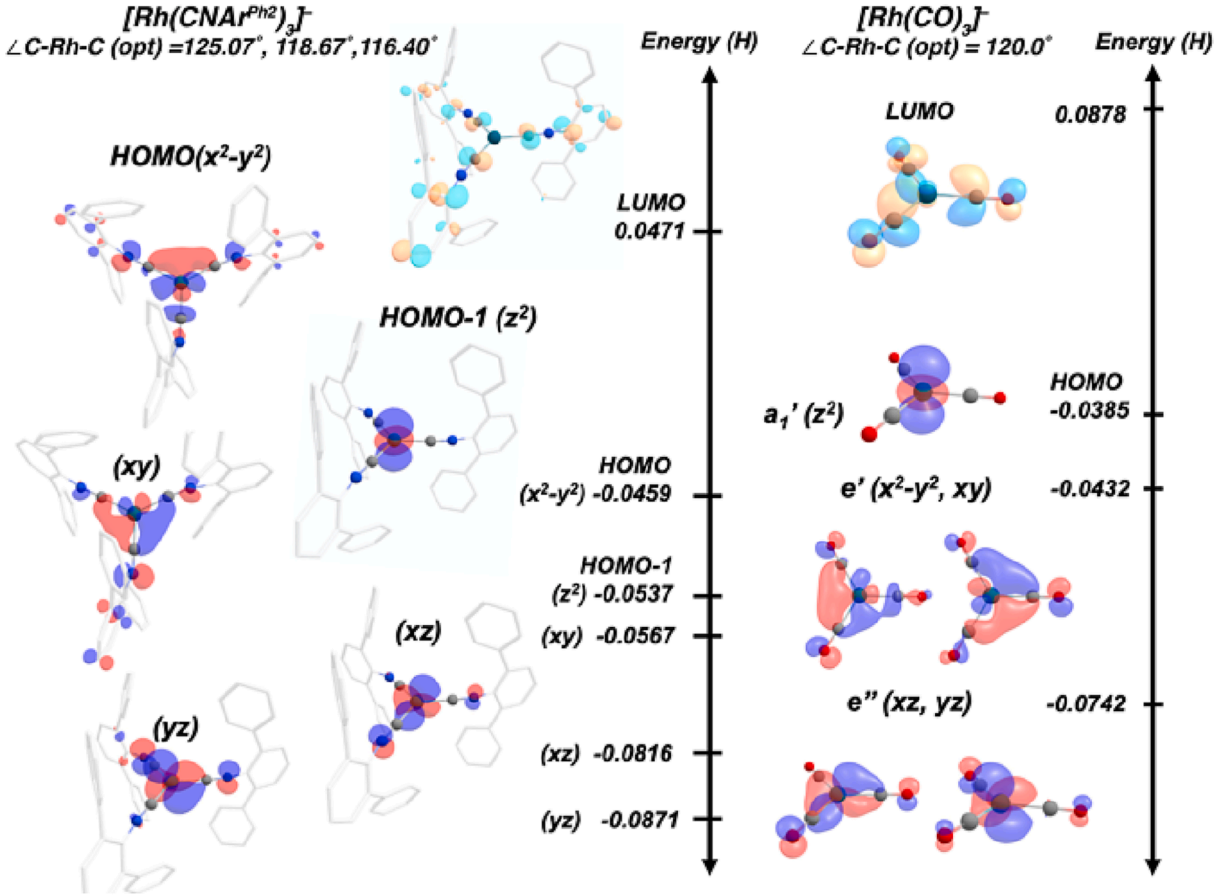

Fig. 2. DFT-calculated (B3LYP/LANL2DZ) molecular orbitals, associated d-orbital splitting pattern and optimized metrical parameters for the C_{2v}-symmetric model complex [Rh(CNAr^{Ph2})$_3$]$^-$ (left) and the D_{3h}-symmetric tricarbonyl metalate [Rh(CO)$_3$]$^-$ (right).

5d metals [31]. However, as the combination of three-coordinate geometries and d^{10} configurations have not been previously established for the heavy Group 9 metals with monodentate ligands [12,13], the observed structural distortion away from D_{3h}-symmetry, where π-backbonding is maximized, can be rationalized in terms of simultaneously maximizing the stability of the σ-bonding framework [33]. In this respect, the anions in [K(crypt)][**3**] and [K(crypt)][**4**] mirror the structural chemistry of the neutral, d^{10} trisphosphine complexes, M$(PPh_3)_3$ (M = Pd, Pt), which also display Y-shaped structural distortions in the solid state [34,35]. Furthermore, it is important to note DFT calculations on the simple tricarbonyl anion, $[Rh(CO)_3]^-$, which has only been observed under matrix isolation conditions [27], optimizes to a D_{3h}-geometry with a HOMO of dz^2 parentage (Fig. 2). Accordingly, this contrasts with the calculated frontier orbtials of $[Rh(CNAr^{Ph2})_3]^-$ and is consistent with the significantly weaker σ-donating properties and greater π-accepting character of CO relative to isocyanides [23,36,37].

Both the K^+ and $[K(crypt)]^+$ salts of metalates [**3**] and [**4**] can be prepared and manipulated under an N_2 atmosphere and show no propensity for N_2 binding. However, the cobalt congener, $[Co(CNAr^{Dipp2})_3]^-$, exhibits distinctly different behavior. As shown in Scheme 2, treatment of $CoCl_2$ with 3.0 equiv of $CNAr^{Dipp2}$ in THF under N_2, followed by addition of sodium amalgam (Na/Hg), results in the isolation of the four-coordinate dinitrogen complex, $Na[Co(N_2)(CNAr^{Dipp2})_3]$ (Na[**5**-N_2]), as determined by X-ray diffraction (Fig. 3). Unlike the synthesis of K[**3**] and K[**4**], repeated attempts to prepare the potassium derivative of [**5**-N_2]$^-$ using KC_8 led to intractable mixtures. Nevertheless, in the solid state, Na[**5**-N_2] exhibits contact ion-pairing between the isocyanide C≡N units and the Na^+ cation, while the terminal N_2 ligand occupies a position distal from the Na center. The solution FTIR spectrum of Na[**5**-N_2] features broad, overlapping ν_{CN} stretches from 2018 to 1840 cm^{-1}, which are indicative of a significantly reduced Co center and contact ion pairing interaction involving the isocyanide C≡N units. Most notably, the FTIR spectrum of Na[**5**-N_2] shows a sharp ν_{NN} band centered at 2159 cm^{-1}. This relatively high-energy band reflects only a marginal degree of NN activation [38], which is unusual given the electron-rich nature of the Co center in Na[**5**-N_2]. While isocyanide ligands are expected to function as stronger π-acids than N_2, and therefore more effectively compete for metal-based electron density, the magnitude of π-backdonation from the Co to the π* (C≡N) orbitals in [**5**-N_2]$^-$ is similar to that of the Rh and Ir metalates K[**3**] and K[**4**]. However, the fact that the anionic $[Co(CNAr^{Dipp2})_3]^-$ unit binds N_2, while the analogous Rh and Ir do not, suggests that the Co center in these metalates retains a far higher degree of Lewis acidity. Lending further credence to this notion is that the unsolvated metalate salt, $Na[Co(CNAr^{Dipp2})_3]^-$ (Na[**5**]), can be prepared via Na/Hg reduction of $CoCl_2$ under an argon atmosphere (Scheme 2). Rather than adopting a three-coordinate geometry, crystallographic analysis revealed the clear presence of a C—H agostic interaction [39] between the Co center and an isopropyl methyl group of the $CNAr^{Dipp2}$ ligand (Fig. 3). In addition, this agostic interaction is located in the apical position of a canonical trigonal monopyramid, which is the coordination geometry expected from coordination of a fourth ligand to the p_z orbital of a d^{10} metal center.

We contend that the enhanced Lewis acidity displayed by $[Co(CNAr^{Dipp2})_3]^-$ is due to the lower energy of the empty Co $4p_z$ orbital relative to the empty $5p_z$ and $6p_z$ orbitals in K[3] and K[4], respectively. Importantly, Lu has described a related phenomenon for the rhodium $[ERhL_3]^-$ metallate complexes (E = Al, Ga, In; L = N(*o*-$(C_6H_4)NCH_2P$(*i*-

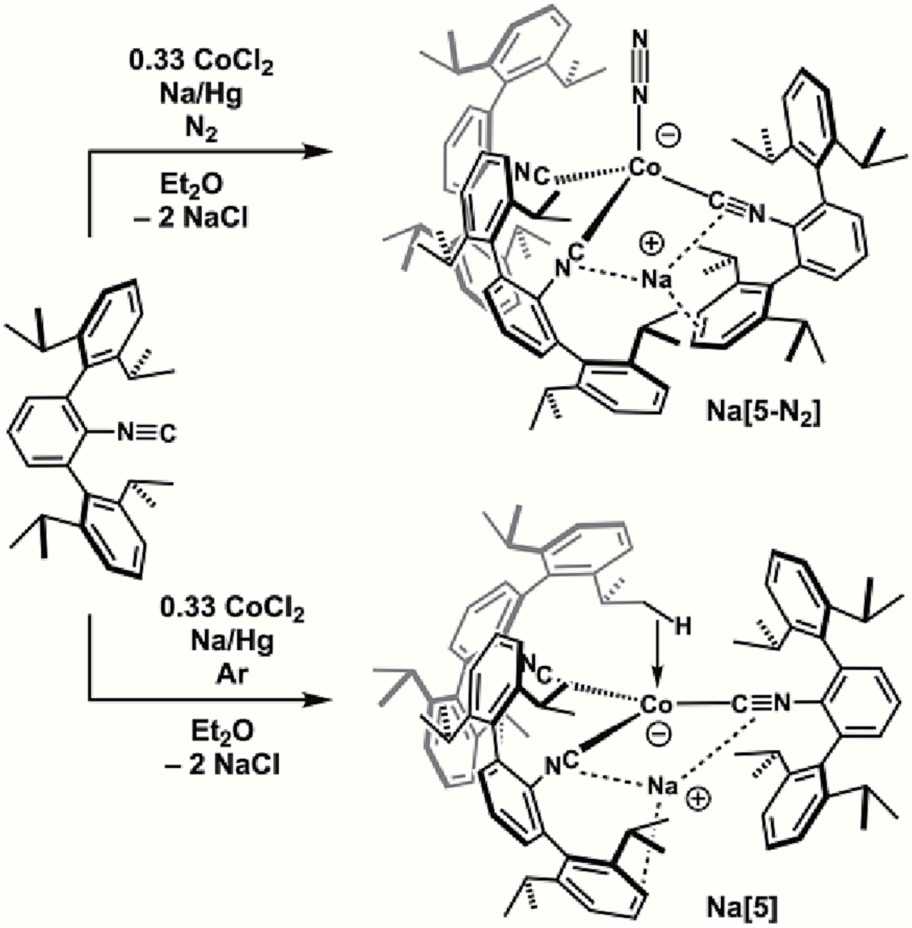

Scheme 2. Synthesis of the cobalt metalate complexes $Na[(N_2)Co(CNAr^{Dipp2})_3]$ (Na[**5**-N_2]) and $Na[Co(CNAr^{Dipp2})_3]$ (Na[**5**]), which possesses a C—H agostic interaction in the solid-state.

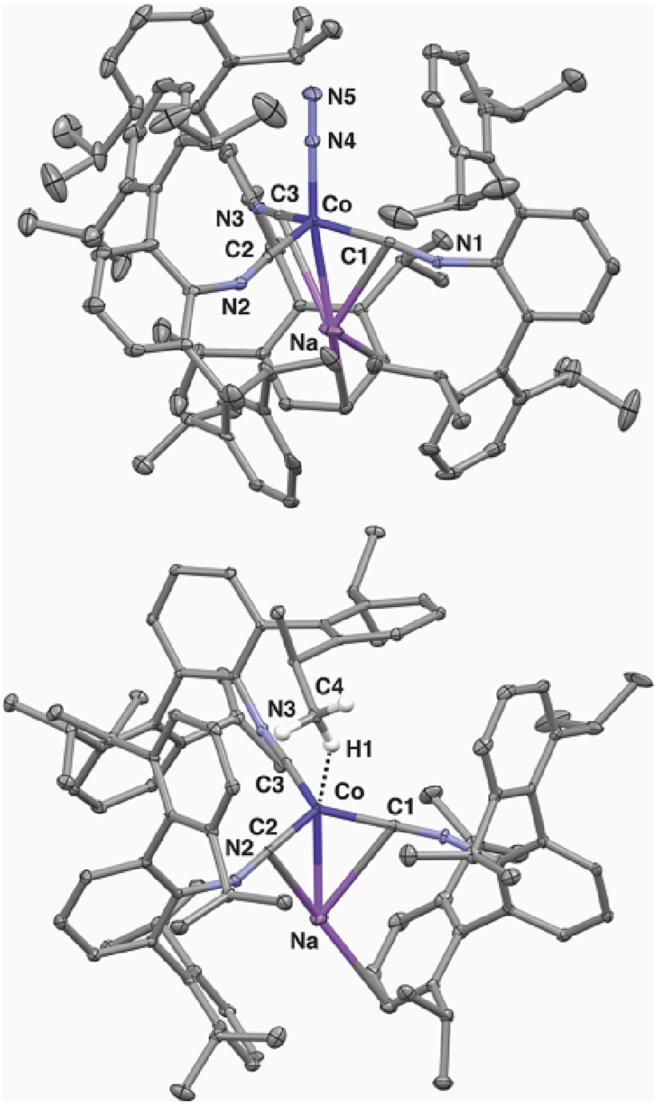

Fig. 3. Molecular structures of the cobalt metalate complexes Na[(N_2)Co$(CNAr^{Dipp2})_3$] (Na[**5**-N_2]; top) and Na[Co$(CNAr^{Dipp2})_3$] (Na[**5**], bottom). Selected Bond Distances for Na[**5**] (Å). d(Co-H1) = 2.009(2); d(Co-C4) = 2.899(13).

$Pr_2))_3$) featuring Lewis-acid coordination to a formally anionic [Rh$(PR_3)_3]^-$ fragment [11]. In that work, coordination of Al and Ga Lewis acids to the Rh center results in four-coordinate structures. However, upon coordination of the more Lewis-acidic indium center to rhodium, a five-coordinate dinitrogen complex is observed, with the N_2 unit bound *trans* to the Lewis acid (*i.e.* Z-type ligand). As has now been established, Lewis-acid coordination to d^{10} metal centers effectively lowers the energy of *trans*-disposed acceptor orbitals of p-orbital parentage [40–45]. This effect has traditionally been evaluated as a function of the acceptor strength of Lewis acidic ligands [44,46]. However, a similar effect can be expected for a transition-metal triad when low-coordination numbers, and therefore, empty metal-based p-orbitals are available. To this end, it is important to note that the Na^+ cation in both Na[5] and Na[**5**-N_2] occupies a position seemingly within bonding contact to the Co center and could in principle function as a *trans*-disposed Z-type ligand. However, the zwitterionic complex [η^2-*C,C*-PPN][Co$(CNAr^{Mes2})_3$] [17], which possesses the less encumbered [Co$(CNAr^{Mes2})_3]^-$ metalate fragment, binds the traditionally non-coordinating $[PPN]^+$ cation, which in turn stabilizes the coordinatively-unsaturated Co center. Coupled with the binding of both N_2 and C—H bonds in Na[**5**] and Na[**5**-N_2], this unusual coordination behavior of [η^2-*C,C*-PPN][Co$(CNAr^{Mes2})_3$], provides additional evidence that the cobalt congener in three-coordinate metalates of the Group 9 triad possess the most significant Lewis acidic properties.

While the coordinatively unsaturated Rh and Ir metalates K[**3**] and K[**4**] do not bind N_2 or coordinating solvents such as THF or Et_2O, we sought to assess whether the coordination of a Z-type ligand could induce such behavior. Previously we demonstrated that binding of Tl(I) ions to the d^{10} nickel tris-isocyanide complex Ni$(CNAr^{Mes2})_3$ results in the π -coordination of a $CNAr^{Mes2}$ ligand mesityl group to the Ni center [42]. This interaction is absent in $16e^-$ Ni$(CNAr^{Mes2})_3$, which adopts a near perfect trigonal planar coordination geometry [32]. As shown in Scheme 3, treatment of the Ir metalate K[**4**] with 1.0 equivalent of thallium triflate (TlOTf; $[OTf]^- = [O_3SCF_3]^-$) under N_2 readily generates the neutral, four-coordinate complex TlIr$(CNAr^{Dipp2})_3$ (**6**) as determined by X-ray diffraction (Fig. 4). In contrast, the Rh derivative K[3] reacts with equimolar TlOTf to afford 0.5 equiv of the bis-thallium salt [Tl_2Rh$(CNAr^{Dipp3})_3$]OTf (**7**), leaving 0.5 equivalent of starting material remaining (Scheme 3; Fig. 4). However, treatment of K[3] with 2.0 equivalents of TlOTf furnishes salt **7** exclusively, which can then be converted to the neutral mono-thallium adduct, TlRh$(CNAr^{Dipp3})_3$ (**8**), by simple addition of potassium iodide (KI) under an N_2 atmosphere (KI; Scheme 3; Fig. S2.11). Notably, mono-thallium adducts **6** and **8** can be viewed as neutral analogues of Lu's anionic Rh/Group 13 element $[ERhL_3]^-$ metalate complexes with respect to the EML_3 unit [11]. Indeed, mono-thallium adducts **6** and **8** give rise to ν_{CN} bands of 2027 cm^{-1} and 1964 cm^{-1}, respectively, which are substantially higher in energy than the ν_{CN} bands of [K(crypt)][**3**] and [K(crypt)][**4**] (1737 cm^{-1} and 1781 cm^{-1} for [**3**]$^-$; 1724 cm^{-1} and 1768 cm^{-1} for [**4**]$^-$), and thus reflect that the Tl(I) ion functions as a Lewis acid and removes electron density from these reduced metal centers [31,32]. Most importantly however, the Ir and Rh centers in complexes **6** and **8**, respectively, adopt trigonal monopyramidal coordination geometries that are free of N_2, bound solvent or secondary interactions from the $CNAr^{Dipp2}$ ligands. As formally Tl(I) centers are reasonably assumed to be less effective Lewis acids than trivalent Group 13 EX_3 species, we interpret these observations as resulting from the inability of Tl(I)-coordination to lower p-orbital energies to a level that enables Lewis base binding. Correspondingly, these findings suggest that $16e^-$ d^{10} Rh and Ir metalates are not as inherently Lewis acidic as their coordinatively-unsaturated nature would indicate.

With respect to the synthesis of complexes **6**–**8**, it is notable that treatment of K[**3**] and K[**4**] with TlOTf provides well defined Tl-adducts without competing $1e^-$ oxidation processes. This behavior contrasts with that of the cobalt-metalate salts, Na[**5**] and Na[**5**-N_2], which are readily oxidized to a multitude of paramagnetic products upon contact with TlOTf. Indeed, K[**3**] and K[**4**] react cleanly with a range of electrophiles in a manner consistent with metalate-type nucleophilic behavior. For example, the Rh metalate K[**3**] reacts readily with trimethylsilyl triflate (Me_3SiOTf) to generate the neutral, monovalent silyl complex Rh$(SiMe_3)(CNAr^{Dipp2})_3$ (**9**) with the elimination of KOTf (Scheme 4). Similarly, both K[**3**] and K[**4**] can be protonated upon treatment with benzoic acid to afford the square planar, d^8 monohydride complexes, HM$(CNAr^{Dipp2})_3$ (M = Rh (**10**); M = Ir (**11**)). Notably, complex **11** represents a rare example of a four-coordinate formally Ir(I) monohydride [47–49], and to our knowledge, its synthesis from K[**4**] and benzoic acid represents a unique protonation-based preparation of such a species. More remarkably however, the nucleophilic reactivity of these three-coordinate Group 9 metalates can also be extended to weakly electrophilic substrates. As shown in Scheme 4, the rhodium derivative K[**3**] reacts with hexamethyldisilane ($Me_3SiSiMe_3$) in THF solution to afford the bis-silyl salt, K[*trans*-Rh$(SiMe_3)_2(CNAr^{Dipp2})_2$] (**12;** Fig. 4), concomitant with the release of one $CNAr^{Dipp2}$ ligand. Oxidative cleavage of Si-Si bonds is well established for zero-valent Pd and Pt complexes but is rare for other metals [50–54]. Most importantly, this nucleophilic behavior of metalates K[**3**] and K[**4**] demonstrate that they can engage

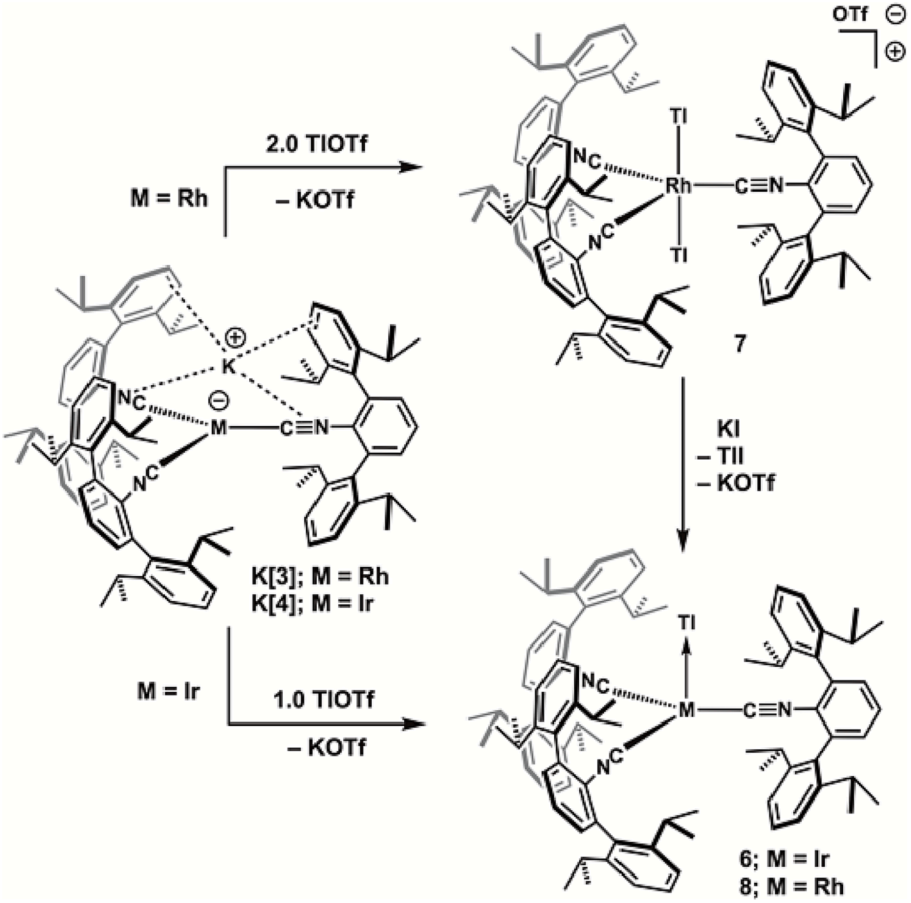

Scheme 3. Tl(I) coordination to Rh and Ir metalate anions.

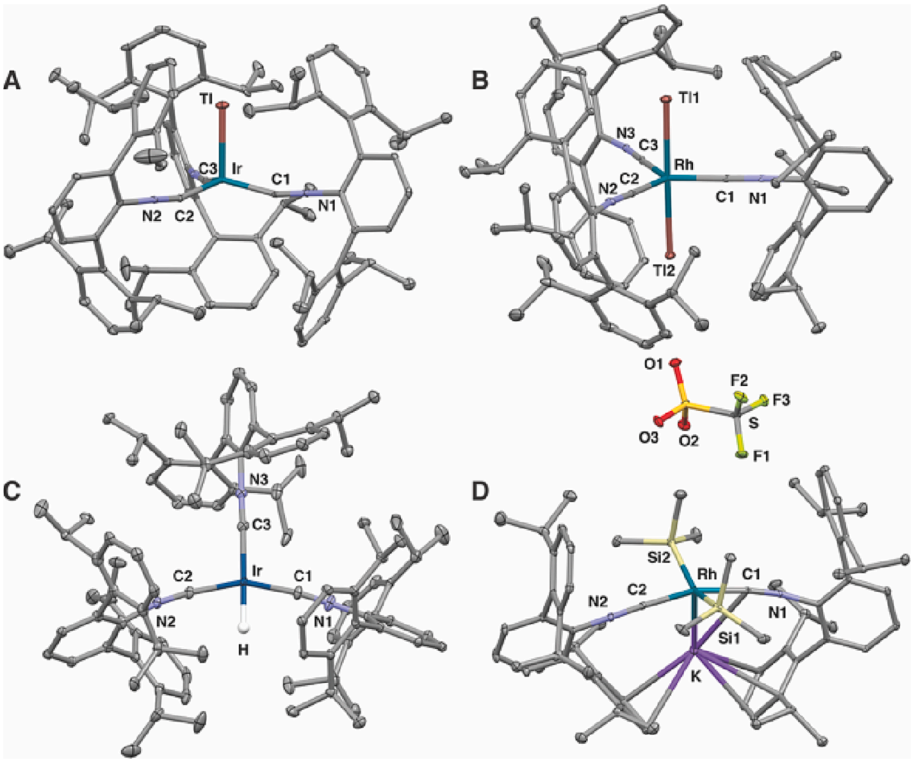

Fig. 4. Molecular structures of (A) $TlIr(CNAr^{Dipp2})_3$ (**6**), (B) $[Tl_2Rh(CNAr^{Dipp2})_3]OTf$ with some isopropyl groups removed for clarity, (C) $HIr(CNAr^{Dipp2})_3$ (**11**) and K $(Rh(SiMe_3)_2(CNAr^{Dpp2})_2]$ (**12**).

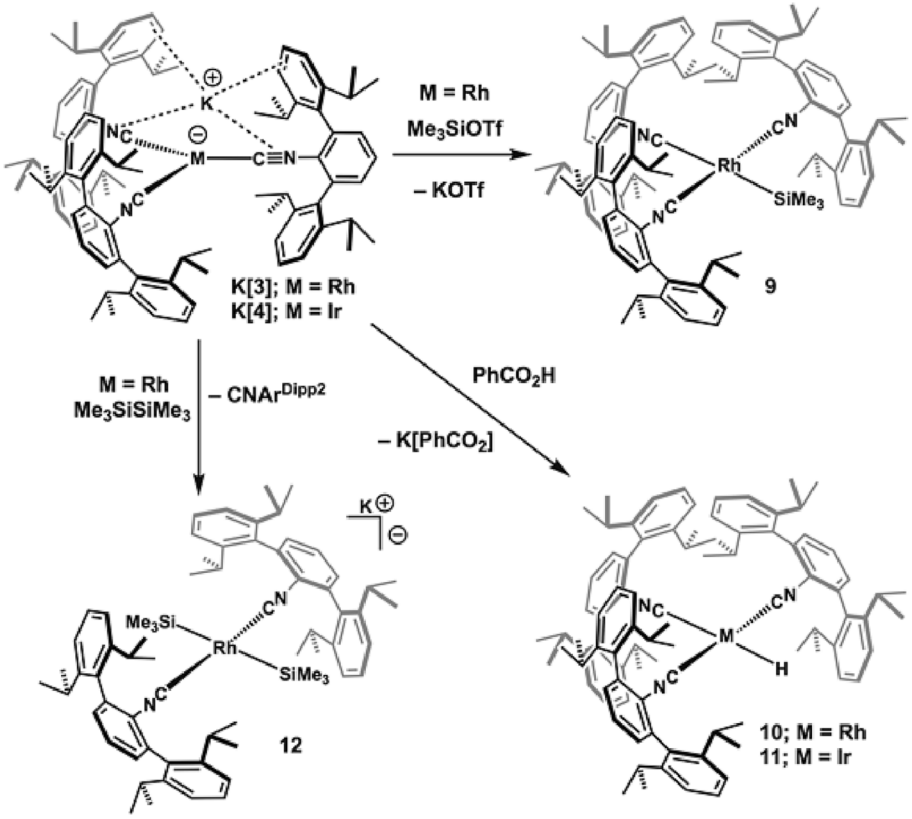

Scheme 4. Nucleophilic behavior of $[M(CNAr^{Dipp2})_3]^-$ metalate anions (M = Rh, Ir).

with substrates along the formal M(1-)/M(I) redox couple. As reactivity utilizing the M(I)/M(III) redox couple is well established for Rh(I) and Ir (I) complexes, access to the formally M(1-) state potentialy offers a path forward for the development of four-electron redox processes using these heavier Group 9 metals.

3. Conclusion

In summary, three-coordinate d^{10} metalate anions of rhodium and iridium are synthetically accessible from the *m*-terphenyl isocyanide ligand, $CNAr^{Dipp2}$. Unexpectedly, despite possessing rigorous coordinative unsaturation, the metalate monoanions of the formualation $[M(CNAr^{Dipp2})_3]^-$ (M = Rh, Ir) are not potent Lewis acids and resist the binding of small molecule substrates such as N_2. However, these heavier Group 9 metalate anions display reactivity properties consistent with presence of electron-rich, nucleophilic metal centers. We are currently pursuing investigations aimed at further exploiting this reactivity profile, as the results reported here demonstrate that reasonably π-acidic ligands and a kinetically stabilizing steric environment can provide a convenient entry point to low-coordinate, yet highly reduced, mononuclear Group 9 metal centers that are competent for "at-metal" nucleophilic behavior.

4. Experimental section

4.1. General considerations

All manipulations were carried out under an atmosphere of purified dinitrogen using standard Schlenk and glovebox techniques. Unless otherwise stated, reagent-grade starting materials were purchased from commercial sources and either used as received or purified by standard procedures [55]. Solvents were dried and deoxygenated according to standard procedures [56]. Benzene-d_6 (Cambridge Isotope Laboratories) was distilled from NaK alloy/benzophenone ketyl and stored over 4 Å molecular sieves under N_2 for at least 24 h prior to use. Celite 405 (Fisher Scientific) was dried under vacuum (24 h) at 250 ℃ and stored in the glovebox prior to use. The m-terphenyl isocyanide $CNAr^{Dipp2}$ was prepared as previously reported [21].

Solution ^1H and $^{13}C\{^1H\}$ NMR spectra were recorded on a Bruker Avance 300, a Varian Mercury 400, a Jeol ECA 500, or a Varian X-SENS 500 spectrometer. ^1H and $^{13}C\{^1H\}$ chemical shifts are reported in ppm relative to $SiMe_4$ (^1H and ^{13}C $\delta = 0.0$ ppm) with reference to residual solvent resonances of 7.16 ppm (^1H) and 128.06 ppm (^{13}C) for C_6D_6 [57]. Solution FTIR spectra were recorded on a Thermo-Nicolet iS10 FTIR spectrometer. Samples were prepared as C_6D_6 solutions injected into a ThermoFisher solution cell equipped with KBr windows. For solution FTIR spectra, solvent peaks were digitally subtracted from all spectra by comparison with an authentic spectrum obtained immediately prior to that of the sample. The following abbreviations were used for the intensities and characteristics of important IR absorption bands: vs = very strong, s = strong, m = medium, w = weak, vw = very weak; b = broad, vb = very broad, sh = shoulder. Combustion analyses were performed by Midwest Microlab LLC, Indianapolis, IN.

4.2. Synthesis of $RhCl(CNAr^{Dipp2})_3$ (1)

$[RhCl(COD)]_2$ (0.619 g, 1.255 mmol, 0.5 equiv) and $CNAr^{Dipp2}$ (3.124 g, 7.533 mmol, 3 equiv) were combined as solids and dissolved in 40 mL of THF. The yellow/orange reaction was stirred at room temperature for 4 h before being dried in vacuo. The resulting yellow solid was slurried 3 times in *n*-pentane for 10 min and dried to remove excess cyclooctadiene. Recrystallization of the solid from a concentrated THF solution followed by storage at –32 °C for 1 week afforded yellow crystals suitable for X-ray diffraction. Yield: 3.01 g, 2.134 mmol, 85%. ^1H NMR (499.8.9 MHz, C_6D_6, 20 ℃): δ = 7.42 (t, 4H, *J* = 8 Hz, *p*-Dipp), 7.29 (d, 8H, *J* = 8 Hz, *m*-Dipp), 7.16 (t, 2H, *J* = 8 Hz, *p*-Dipp), 7.12 (d,

4H, $J = 8$ Hz, *m*-Dipp), 6.93 (d, 4H, $J = 8$ Hz, *m*-Ar), 6.89 (d, 2H, $J = 8$ Hz, *m*-Ar), 6.83 (dd, 2H, $J = 8$ Hz, *p*-Ar), 6.79 (dd, 1H, $J = 8$ Hz, *p*-Ar), 2.73 (septet, 8H, $J = 7$ Hz, C*H*$(CH_3)_2$), 2.54 (septet, 4H, $J = 7$ Hz, C*H*$(CH_3)_2$), 1.27 (d, 24H, $J = 7$ Hz, C*H*$(CH_3)_2$), 1.10 (d, 24H, $J = 7$ Hz, C*H*$(CH_3)_2$), 1.09 (d, 12H, $J = 7$ Hz, CH(C*H*$_3)_2$), 0.96 (d, 12H, $J = 7$ Hz, CH(C*H*$_3)_2$) ppm. $^{13}C\{^1H\}$ NMR (125.8 MHz, C_6D_6, 20 ℃): $\delta = 163.3$ (d, $J_{CRh} = 70.2$ Hz, *C*NR), 159.6 (d, $J_{CRh} = 58.8$ Hz, *C*NR), 147.5, 146.7, 138.1, 137.9, 135.7, 135.4, 131.6, 130.9, 129.6, 129.4, 127.8, 127.5, 127.2, 126.1, 123.6, 31.2, 31.0, 25.4, 24.8, 24.6 ppm. FTIR (KBr windows, C_6D_6, 20 ℃) ν (C≡N) = 2152 (w), 2094 (vs), 2059 (s), 2036 (s), 2001(s) cm^{-1}; also 3062 (w) 3062 (w), 2962 (s), 2927 (m), 2865 (m), 1577 (w), 1457 (m), 1411 (w), 1384 (w), 1361 (w), 1056 (w), 759 (s) cm^{-1}. Anal. calcd. for $C_{93}H_{111}N_3Rh_1Cl_1$: C, 79.26; H, 7.94; N, 2.98. Found: C, 79.58; H, 8.09; N, 3.02.

4.3. Synthesis of IrCl(CNAr^{Dipp2})$_3$ (2)

The procedure for RhCl(CNAr^{Dipp2})$_3$ (1) was followed using [IrCl(COD)]$_2$ (0.842 g, 1.253 mmol, 0.5 equiv). Recrystallization of the resulting red solid from *n*-pentane spiked with 2 drops of Et_2O (5 mL total) followed by storage at –32 °C for 1 week afforded red crystals suitable for X-ray diffraction. Yield: 3.21 g, 2.15 mmol, 86%. ^1H NMR (499.8.9 MHz, C_6D_6, 20 ℃): δ = 7.41 (t, 4H, $J = 8$Hz, *p*-Dipp), 7.27 (d, 8H, $J = 8$ Hz, *m*-Dipp), 7.16 (t, 2H, $J = 8$ Hz, *p*-Dipp), 7.11 (d, 4H, $J = 8$ Hz, *m*-Dipp), 7.04 (t, 2H, $J = 8$ Hz, *m*-Ar), 6.89 (d, 2H, $J = 8$ Hz, *m*-Ar), 6.81 (t, 2H, $J = 8$ Hz, *p*-Ar), 6.80 (t, 1H, $J = 8$ Hz, *p*-Ar), 2.71 (septet, 8H, $J = 7$ Hz, C*H*$(CH_3)_2$), 2.57 (septet, 4H, $J = 7$ Hz, C*H*$(CH_3)_2$), 1.26 (d, 24H, $J = 7$ Hz, CH(C*H*$_3)_2$), 1.10 (d, 24H, $J = 7$ Hz, CH(C*H*$_3)_2$), 1.09 (d, 12H, $J = 7$ Hz, CH(C*H*$_3)_2$), 0.98 (d, 12H, $J = 7$ Hz, CH(C*H*$_3)_2$) ppm. $^{13}C\{^1H\}$ NMR (125.8 MHz, C_6D_6, 20 C): δ = 154.2 (CNR), 151.1 (CNR), 147.0, 146.4, 138.1, 137.0, 135.9, 135.0, 131.2, 130.6, 130.2, 129.2, 128.8, 127.3, 127.2, 126.8, 124.9, 123.2, 123.0, 30.8, 30.6, 29.9, 25.0, 24.6, 24.3, 24.2 ppm. FTIR (KBr windows, C_6D_6, 20 ℃) υ(C≡N) = 2156 (w), 2082 (vs), 1967 (s) cm^{-1}; also 2962 (s), 2927 (m), 2865 (m), 1577 (w), 1461 (m), 1411 (w), 1384 (w), 1361 (w), 759 (m) cm^{-1}. Anal. calcd. for $C_{93}H_{111}N_3IrCl$: C, 74.54; H, 7.47; N, 2.37. Found: C, 75.68; H, 7.47; N, 2.49.

4.4. Synthesis of K[Rh(CNAr^{Dipp2})$_3$] (K[3])

To a thawing 1:2 Et_2O/THF solution (20 mL total) of RhCl(CNAr-^{Dipp2})$_3$ (**1**; 0.300 g, 0.213 mmol, 1 equiv) was added KC_8 (0.086 g, 0.639 mmol, 3 equiv.) in two equal portions, letting the reaction stir at −32 °C for 30 min between additions. After the second addition, the reaction mixture was allowed stir for an additional 30 min at −32 ℃ before filtering over Celite to remove graphite and KCl. The resulting dark brown filtrate was dried in vacuo before being subjected to three cycles of slurrying in *n*-pentane (3 × 5 mL) to remove any remaining THF. The resultant dark solid was dissolved in C_6H_6 and filtered over a plug of Celite packed on fiberglass. The filtrate was frozen and lyophilized to a fluffy powder. Yield: 0.285 g, 0.202 mmol, 95%. Recrystallization of the solid from *n*-pentane spiked with 3 drops of Et_2O (5 mL total) followed by storage at −32 °C for 3 weeks afforded dark red crystals suitable for X-ray diffraction. ^1H NMR (499.8.9 MHz, C_6D_6, 20 ℃): δ = 7.28 (t, 6H, $J = 8$ Hz, *p*-Dipp), 7.17 (d, 12H, $J = 8$ Hz, *m*-Dipp), 6.96 (d, 6H, $J = 8$ Hz, *m*-Ar), 6.88 (t, 3H, $J = 8$ Hz, *p*-Ar), 2.86 (septet, 12H, $J = 7$ Hz, C*H*$(CH_3)_2$), 1.18 (d, 36H, $J = 7$ Hz, CH(C*H*$_3)_2$), 1.14 (d, 36H, $J = 7$ Hz, CH(C*H*$_3)_2$) ppm. $^{13}C\{^1H\}$ NMR (125.8 MHz, C_6D_6, 20 ℃): δ = 212.9 (d, $J_{C\text{-}Rh} = 82.3$ Hz, *C*NR), 147.8, 138.3, 135.2, 133.4, 130.2, 128.7, 123.1, 31.0, 25.1, 24.3 ppm. FTIR (KBr windows, C_6D_6, 20 ℃) υ(C≡N) = 2067 (w), 2012 (m, sh), 1982 (vs), 1850 (s, br), 1741 (s, br), 1688 (vs), cm^{-1}; also 2962 (s), 2962 (m), 1866 (m), 1461 (m), 1411 (s), 1383 (w), 1362 (w), 1328 (s), 1199 (w), 1177 (w), 1055 (m, br), 757 (s) cm^{-1}. Anal. calcd. for $C_{93}H_{111}N_3RhK$: C, 79.06; H, 7.92; N, 2.97. Found: C, 78.68; H, 7.80; N, 2.87.

4.5. Synthesis of K[Ir(CNAr^{Dipp2})$_3$] (K[4])

To a thawing 1:2 Et_2O/THF mixture of IrCl(CNAr^{Dipp2})$_3$ (**2**; 0.126 g, 0.084 mmol, 1 equiv, 15 mL) was added KC_8 (0.034 g, 0.252 mmol, 3 equiv) in two equal portions, letting the reaction stir at −32 ℃ for 30 min between additions. After the second addition, the reaction was allowed to stir for an additional 30 min at −32 ℃ before filtering over Celite packed remove both graphite and KCl. The resulting dark brown filtrate was dried in vacuo before being subjected to three cycles of slurrying in *n*-pentane (3 × 5 mL) and drying in vacuo to remove any remaining THF. The resultant dark solid was dissolved in C_6H_6 and filtered over Celite. The filtrate was frozen and lyophilized to a fluffy powder. Yield: 0.115 g, 0.077 mmol, 91%. Recrystallization of the solid from *n*-pentane spiked with 2 drops of Et_2O (3 mL total) followed by storage at −32 C for 1 week afforded dark red crystals suitable for X-ray diffraction. ^1H NMR (499.8.9 MHz, C_6D_6, 20 ℃): δ = 7.26 (t, 6H, $J = 8$ Hz, *p*-Dipp), 7.18 (d, 12H, $J = 8$ Hz, *m*-Dipp), 7.00 (d, 6H, $J = 8$ Hz, *m*-Ar), 6.92 (t, 3H, $J = 8$ Hz, *p*-Ar), 2.9 (septet, 12H, $J = 7$ Hz, C*H*$(CH_3)_2$), 1.18 (d, 36H, $J = 7$ Hz, CH(C*H*$_3)_2$), 1.13 (d, 36H, $J = 7$ Hz, CH(C*H*$_3)_2$) ppm. $^{13}C\{^1H\}$ NMR (125.8 MHz, C_6D_6, 20 ℃): δ = 225.5 (*C*NR), 147.7, 138.4, 137.0, 133.0, 130.3, 128.8, 123.1, 122.7, 31.0, 25.1, 24.2 ppm. FTIR (KBr windows, C_6D_6, 20 ℃) υ(C≡N) = 2015 (m, sh), 1961 (s), 1804 (vs, sh), 1743 (vs), 1657 (vs), 1660 (vs, sh) cm^{-1}; also 3060 (m), 3038(w, sh), 3022 (w, sh), 2962 (s), 2926 (m), 2866 (m), 1571 (vs), 1461 (s), 1411 (s), 1383 (m), 131 (m), 1331 (s), 1251 (w), 1202 (w), 1177 (w), 1055 (m), 924 (w), 795 (s), 680 (m), 620 (w), 582 (m), 570 (m) cm^{-1}. Anal. calcd. for $C_{93}H_{111}N_3IrK$: C, 74.36; H, 7.45; N, 2.80. Found: C, C, 73.90; H, 7.38; N, 3.23.

4.6. Synthesis of [K(cryptand-2.2.2)][Rh(CNAr^{Dipp2})$_3$] ([K(crypt)][3])

To a stirring solution of K[Rh(CNAr^{Dipp2})$_3$] (K[**3**]; 0.027 g, 0.019 mmol, 1 equiv) in 2 mL C_6H_6, cryptand-2.2.2 (0.006 g, 0.015 mmol, 1 equiv) was added as a solid. The reaction was allowed to stir 20 min, during which time a dark precipitate formed. The precipitate was collected via filtration on a pad of Celite, and washed with *n*-pentane (3 × 2 mL). The precipitate was then dissolved and washed through the Celite with 5 mL of THF. The THF filtrate was the dried in vacuo yielding a dark red solid. Yield: 0.032 g, 0.018 mmol, 93%. X-ray quality crystals were grown by dissolving the solid in 2 mL of a THF/benzene (20:1) solution and placing it at −32 C for 2 weeks. ^1H NMR (499.8.9 MHz, C_6D_6, 20 ℃): δ = 7.28 (t, 6H, 8 J = Hz, *p*-Dipp), 7.17 (d, 12H, $J = 8$ Hz, *m*-Dipp), 6.96 (d, 6H, $J = 8$ Hz, *m*-Ar), 6.88 (t, 3H, $J = 8$ Hz, *p*-Ar), 3.57 (s, 12H, CH_2CH_2O), 3.53 (dd, 12H, OCH_2CH_2N), 2.55 (s, 12H), OCH_2CH_2N), 2.86 (septet, 12H, $J = 7$ Hz, C*H*$(CH_3)_2$), 1.18 (d, 36H, $J = 7$ Hz, CH(C*H*$_3)_2$), 1.14 (d, 36H, $J = 7$ Hz, CH(C*H*$_3)_2$) ppm. $^{13}C\{^1H\}$ NMR (125.8 MHz, C_6D_6, 20 ℃): δ = 212.9 (d, $J_{CRh} = 86.8$ Hz, *C*NR), 147.8, 138.3, 135.2, 133.4, 130.2, 128.7, 123.1, 31.0, 25.1, 24.3 ppm. FTIR (KBr windows, THF, 20 C) υ(C≡N) = 1926 (w), 1781 (vs), 1737 (vs) cm^{-1}; also 1569 (s), 1407 (s), 1380 (w, sh), 1355 (m), 1133 (m), 1108 (s), 755 (s) cm^{-1}. Anal. calcd. for $C_{111}H_{147}N_5O_6RhK$: C, 74.51; H, 8.24; N, 3.91. Found: C, 74.36; H, 8.34; N, 3.90.

4.7. Synthesis of [K(cryptand-2.2.2)][Ir(CNAr^{Dipp2})$_3$] ([K(crypt)][4])

This compound was prepared and crystallized analogously to K(crypt)[**3**] using 0.023 g of K[Ir(CNAr^{Dipp2})$_3$] (K[**4**]; 0.017 mmol, 1 equiv) and 0.006 g of cryptand-2.2.2 (0.015 mmol, 1 equiv). Yield (dark red solid): 0.030 g, 0.016 mmol, 92%. ^1H NMR (499.8.9 MHz, THF-d^8, 20 ℃): δ = 7.30 (t, 3H, $J = 8$ Hz, p-Ar), 7.03 (t, 6H, $J = 8$ Hz, *p*-Dipp), 6.90 (d, 12H, $J = 8$ Hz, m-Dipp), 6.74 (d, 6H, $J = 8$ Hz, *m*-Ar), 3.64 (septet, 12H, $J = 7$ Hz, C*H*$(CH_3)_2$), 3.60 (s, 12H, CH_2CH_2O), 3.53 (dd, 12H, OCH_2CH_2N), 2.54 (s, 12H), OCH_2CH_2N), 0.87 (d, 36H, $J = 7$ Hz, CH(C*H*$_3)_2$), 0.84 (d, 36H, $J = 7$ Hz, CH(C*H*$_3)_2$) ppm. $^{13}C\{^1H\}$ NMR (125.8 MHz, THF-d_8, 20 ℃): δ = 229.1(*C*NR), 147.5, 139.2, 132.7, 129.9, 128.8, 127.5, 122.6, 119.4, 71.1, 68.2, 53.5, 31.1, 30.8, 25.2, 24.8, 24.4

ppm. FTIR (KBr windows, THF, 20 ℃) υ(C≡N) = 1918 (w), 1768 (vs), 1724 (vs), cm^{-1}; also 1569 (s), 1479 (s), 1407 (s), 1355 (m), 752 (m), 680 (s) cm^{-1}. Anal. calcd. for $C_{111}H_{147}N_5O_6IrK$: C, 70.96; H, 7.89; N, 3.73. Found: C, 70.58; H, 7.88; N, 3.48.

4.8. Synthesis of Na[(N_2)Co($CNAr^{Dipp2}$)$_3$] (Na[5-N_2])

This reaction procedure is carried out under $N_{2(g)}$ atmosphere. To a THF (10 mL) suspension of $CoCl_2$ (0.054 g, 0.42 mmol, 1 equiv) was added $CNAr^{Dipp2}$ (0.500 g, 1.26 mmol, 3 equiv). The resulting mixture was allowed to stir for 10 min, after which 0.1 % NaHg (Na: 0.96 g, 4.2 mmol, 10 equivalents; Hg: 9.6 g) was added. The reaction mixture was shaken by hand for ca. 7 min, where upon a color change to deep purple was observed. The reaction mixture was allowed to stir for an additional 20 mins upon which time the solution was decanted from the sodium amalgam via filtration over Celite packed on a medium porosity glass sintered frit and evaporated to dryness. The resulting residue was then slurred in *n*-pentane (15 mL) allowed to stir for 5 min and then concentrated to dryness. This step was repeated two additional times to desolvate residual NaCl by-products, whereupon a color change from purple to red was observed. Extraction of the resulting residue with benzene (10 mL), followed by filtration through Celite produced a deep-red solid. Na[(N_2)Co($CNAr^{Dipp2}$)] is isolated as a fluffy red solid, 0.400 g, 0.29 mmol, 69 % yield. ^{1}H NMR (499.9 MHz, C_6D_6, 20 ℃): δ = 7.31 (t, 6H, *J* = 5 Hz, *p*-Dipp), 7.18 (d, 12H, *J* = 5 Hz, *m*-Dipp), 6.98 (d, 6H, *J* = 5 Hz, *m*-Ph), 6.87 (t, 3H, *J* = 5 Hz, *p*-Ph), 2.91 (septet, *J* = 5 Hz, 12H, C*H*(CH_3)$_2$), 1.27 (d, *J* = 5 Hz, 36H, CH(C*H*$_3$)$_2$), 1.13 (d, *J* = 5 Hz, 36H, CH(C*H*$_3$)$_2$) ppm. ^{13}C{^{1}H} NMR (125.7 MHz, C_6D_6, 20 ℃): δ = 147.5, 138.5, 135.1, 134.0, 130.7, 130.4, 128.6, 127.7, 127.5, 123.1, 34.4, 31.1, 25.4, 24.3, 22.8, 14.3 ppm. Note: The CNR resonance is extremely broadened, presumably due to coupling to ^{59}Co (I = 7/2, 100 %). FTIR (C_6D_6, KBr windows, 25 ℃): ν_{NN} = 2159 (m) cm^{-1}, ν_{CN} = 2018 (w), 1946 (m), 1840 (vs) cm^{-1}, also 2961 (s), 2927 (m), 2868 (w), 1463 (m), 1383 (w), 1363 (w) cm^{-1}. Anal. Calcd. for $C_{93}H_{111}N_3CoNa$: C, 80.89; H, 8.10; N, 5.07. Found C, 80.46; H, 8.28; N, 5.06.

4.9. Synthesis of Na[Co($CNAr^{Dipp2}$)$_3$] (Na[5])

The synthesis of K[**4**] was performed with identical amount and in the same fashion as that of Na[(N_2)Co($CNAr^{Dipp2}$)$_3$] (Na[**5**-N_2]), with the exception that all manipulations were conducted in an argon-filled glovebox. Na[Co($CNAr^{Dipp2}$)$_3$] is isolated as a fluffy deep-red solid, 0.300 g, 0.22 mmol, 52 % yield. ^{1}H NMR (499.9 MHz, C_6D_6, 20 ℃): δ = 7.27 (t, 6H, *J* = 5 Hz, *p*-Dipp), 7.15 (d, 12H, *J* = 5 Hz, *m*-Dipp), 6.94 (d, 6H, *J* = 5 Hz, *m*-Ph), 6.86 (t, 3H, *J* = 5 Hz, *p*-Ph), 2.89 (septet, *J* = 5 Hz, 12H, C*H*(CH_3)$_2$), 1.15 (d, *J* = 5 Hz, 36H, CH(C*H*$_3$)$_2$), 1.02 (d, *J* = 5 Hz, 36H, CH(C*H*$_3$)$_2$) ppm. ^{13}C{^{1}H} NMR (125.7 MHz, C_6D_6, 20 ℃): δ = 205.6 (CNR), 147.8, 138.6, 134.6, 132.6, 130.4, 128.6, 128.4, 127.9, 121.6, 31.2, 25.0, 23.9 ppm. FTIR (C_6D_6, KBr windows, 25 C): ν_{CN} = 2068 (w), 2018 (m), 1934 (vs), 1815 (s) cm^{-1}, also 2961 (s), 2927 (m), 2868 (w), 1463 (m), 1383 (w), 1363 (w) cm^{-1}. Elemental analysis was not preformed due to sensitivity towards N_2.

4.10. Synthesis of TlIr($CNAr^{Dipp2}$)$_3$ (6)

An Et_2O solution of K[Ir($CNAr^{Dipp2}$)$_3$] (K[**3**]; 0.049 g, 0.032 mmol, 1 equiv, 2 mL) was added to a thawing slurry of TlOTf in Et_2O (0.011 g, 0.032 mmol, 1 equiv, 2 mL). The reaction was left to stir and warm to room temperature for 1 hr before being filtered through Celite. The resulting filtrate was then evaporated to dryness in vacuo, leaving TlIr($CNAr^{Dipp2}$)$_3$ (**6**) as a green powder. Yield: 0.050 g, 0.030 mmol, 94%. Recrystallization of the solid from a 3 mL Et_2O solution at −32 C for 2 days afforded green crystals suitable for X-ray diffraction. ^{1}H NMR (499.8.9 MHz, C_6D_6, 20 ℃): δ = 7.28 (t, 6H, *J* = 8 Hz, *p*-Dipp), 7.17 (d, 12H, *J* = 8 Hz, *m*-Dipp), 7.03 (d, 6H, *J* = 8 Hz, *m*-Ar), 6.90 (t, 3H, *J* = 8 Hz, *p*-Ar), 2.84 (septet, 12H, *J* = 7 Hz, C*H*(CH_3)$_2$), 1.15 (d, 36H, *J* = 7 Hz, CH(C*H*$_3$)$_2$), 1.14 (d, 36H, *J* = 7 Hz, CH(CH_3)$_2$) ppm. ^{13}C{^{1}H} NMR (125.8 MHz, C_6D_6, 20 ℃): δ = 180.4 (*C*NR), 147.6, 137.3, 134.1, 133.4, 130.5, 128.4, 123.5, 123.0, 31.1, 25.2, 25.1 ppm. FTIR (KBr windows, C_6D_6, 20 ℃) υ(C≡N) = 2027 (m, sh), 1996 (m, sh), 1896 (vs) cm^{-1}; also 2962 (s), 2926 (m), 2866, (m), 1615 (w), 1576 (m), 1459 (m), 1410 (m), 1383 (w), 1362, (w), 759 (m), 680 (w) cm^{-1}. Anal. calcd. for $C_{93}H_{111}N_3IrTl$: C, 66.99; H, 6.71; N, 2.52. Found: C, 66.64; H, 6.95; N, 2.45.

4.11. Synthesis of [Tl_2Rh($CNAr^{Dipp2}$)$_3$]OTf (7)

An Et_2O solution of K[Rh($CNAr^{Dipp2}$)$_3$] (K[**3**]; 0.096 g, 0.068 mmol, 1 equiv) was added to a stirring slurry of TlOTf in THF (0.053 g, 0.150 mmol, 2.2 equiv). The reaction was left to stir for 24hr before being dried in vacuo. The reaction was then subjected to three cycles of slurrying in *n*-pentane (3 × 5 mL) to remove any remaining THF. The resultant solid was slurried in 30 mL of *n*-pentane and filtered over Celite. The remaining solid and Celite was extracted with 30 mL of Et_2O then dried in vacuo. The resultant powder was dissolved in 2 mL of toluene, and 2 mL of *n*-pentane was layered on top. The solution was allowed to sit for 24 h at −32 ℃ to give forest green, X-ray quality crystals, which were rinsed with minimal amounts of *n*-pentane. Yield: 0.027 g, 0.014 mmol, 21%. ^{1}H NMR (499.8.9 MHz, C_6D_6, 20 ℃): δ = 7.79 (t, 6H, *J* = 8 Hz, *p*-Dipp), 7.41 (d, 12H, *J* = 8 Hz, *m*-Dipp), 6.92 (d, 6H, *J* = 8 Hz, *m*-Ar), 6.86 (t, 3H, *J* = 8 Hz, *p*-Ar), 2.69 (septet, 12H, *J* = 7 Hz, C*H*(CH_3)$_2$), 1.19 (d, 36H, *J* = 7 Hz, CH(C*H*$_3$)$_2$), 1.07 (d, 36H, *J* = 7 Hz, CH(C*H*$_3$)$_2$) ppm. ^{13}C{^{1}H} NMR (125.8 MHz, C_6D_6, 20 ℃): δ = 147.5, 136.2, 135.7, 131.4, 130.4, 125.4, 124.2, 31.2, 24.8, 24.7 ppm. Note, repeated scanning failed to locate the isocyanide ^{13}C resonances. Presumably this is a manifestation of higher order coupling between ^{103}Rh and ^{203}Tl/^{205}Tl. FTIR (KBr windows, C_6D_6, 20 ℃) υ(C≡N) = 2034, (m, sh), 2004 (s, sh), 1967 (vs) cm^{-1}; also 1577 (w), 1462 (m), 1409 (m), 1384 (w), 1363 (w), 1328 (s), 1291 (m), 1240 (s), 1157 (m), 1056 (w), 1026 (s), 761 (m), 680 (w), 637 (m) cm^{-1}. Satisfactory combustion analysis was not obtained after repeated attempts.

4.12. Synthesis of TlRh($CNAr^{Dipp2}$)$_3$ (8)

To a stirring Et_2O/THF (1:5) solution of [Tl_2Rh($CNAr^{Dipp2}$)$_3$]OTf (**7**; 0.145 g, 0.075 mmol, 1 equiv), KI was added as a solid (0.062 g, 0.375 mmol, 5 equiv) and was left to stir for 4 days. The volatiles were then removed in vacuo. The dark residue was then eluted through a 5 cm thick plug of Celite with *n*-pentane, collecting only the dark fraction. Drying the *n*-pentane solution in vacuo yields **8** as a dark green solid. Yield: 0.012 g, 0.008 mmol, 11%. Recrystallization of the solid from a 2 mL *n*-pentane solution spiked with 1 drop of Et_2O at − 32 °C for 5 days afforded dark green crystals suitable for X-ray diffraction. ^{1}H NMR (499.8.9 MHz, C_6D_6, 20 ℃): δ = 7.45 (t, 6H, *J* = 8 Hz, *p*-Dipp), 7.35 (d, 12H, *J* = 8 Hz, *m*-Dipp), 6.99 (t, 3H, *J* = 8 Hz, *p*-Ar), 6.90 (d, 6H, *J* = 8 Hz, *m*-Ar), 2.95 (septet, 12H, *J* = 7 Hz, C*H*(CH_3)$_2$), 1.52 (d, 36H, *J* = 7 Hz, CH(C*H*$_3$)$_2$), 1.23 (d, 36H, *J* = 7 Hz, CH(C*H*$_3$)$_2$) ppm. ^{13}C{^{1}H} NMR (125.8 MHz, C_6D_6, 20 ℃): δ = 147.6, 137.3, 134.1, 133.4, 130.5, 128.4, 123.5, 123.0, 31.1, 25.2, 25.1 ppm. Note, repeated scanning failed to locate the isocyanide ^{13}C{^{1}H} resonances. Presumably this is a manifestation of higher order coupling between ^{103}Rh and ^{203}Tl/^{205}Tl. FTIR (KBr windows, Et_2O, 20 ℃) υ(C≡N) = 2033 (w), 1964 (vs) cm^{-1}; also 2960 (m), 2924 (w), 2867 (w), 1578 (w), 1462 (w), 1413 (m), 1361 (w), 1328 (s), 1178 (m), 1045 (m, br), (758 (m), 680 (m) cm^{-1}. Satisfactory combustion analysis was not obtained after repeated attempts.

4.13. Synthesis of Rh(TMS)($CNAr^{Dipp2}$)$_3$ (9)

To a stirring solution of K[Rh($CNAr^{Dipp2}$)$_3$] (K[**3**]; 0.035 g, 0.025 mmol, 1 equiv) in 3 mL of C_6H_6, trimethylsilyl triflate (Me_3SiOTf; 4.5 μL, 0.025 mmol, 1 equiv) was added dropwise with a 10 μL syringe. The reaction mixture was allowed to stir for 20 min, gradually changing in

color from red to dark green. The reaction mixture was then filtered through Celite, and the resulting filtrate dried in vacuo. X-ray quality crystals were grown by dissolving the resulting solid in 3 mL of a *n*-pentane/benzene (20:1) solution and placing it at −32 ℃ for 3 d. Yield: 0.013 g, 0.010 mmol, 42%. ^{1}H NMR (499.8.9 MHz, C_6D_6, 20 ℃): δ = 7.32 (t, 2H, *J* = 8 Hz, *p*-Dipp), 7.22 (d, 8H, *J* = 8 Hz, *m*-Dipp), 7.15 (d, 4H, *J* = 8 Hz, *m*-Dipp), 7.09 (t, 4H, *J* = 8 Hz, *p*-Dipp), 6.98 (dd, 4H, *J* = 8 Hz, *m*-Ar), 6.97 (dd, 2H, *J* = 8 Hz, *p*-Ar), 6.95 (d, 2H, *J* = 8 Hz, *m*-Ar), 6.93 (t, 1H, *J* = 8 Hz, *p*-Ar), 2.76 (septet, 8H, *J* = 7 Hz, C*H*(CH$_3$)$_2$), 2.70 (septet, 4H, *J* = 7 Hz, CH(C*H*$_3$)$_2$), 1.39 (d, 24H, *J* = 7 Hz, CH(C*H*$_3$)$_2$), 1.29 (d, 12H, *J* = 7 Hz, CH(C*H*$_3$)$_2$), 1.12 (d, 24H, *J* = 7 Hz, CH(C*H*$_3$)$_2$), 1.09 (d, 12H, *J* = 7 Hz, CH(C*H*$_3$)$_2$), 0.04 (s, 9H, Si(C*H*$_3$)$_3$) ppm. ^{13}C{^{1}H} NMR (125.8 MHz, C_6D_6, 20 ℃): δ = 147.0 (*C*NR), 146.7 (*C*NR), 139.5, 138.5, 135.3, 134.9, 130.1, 129.7, 129.5, 127.6, 126.9, 126.6, 123.4, 122.6, 35.5, 31.5, 31.4, 30.3, 24.9, 24.5, 24.3, 24.2, 22.8, 14.3, 9.2 ppm. FTIR (KBr windows, C_6D_6, 20 ℃) υ(C≡N) = 2073 (s), 2023 (s), 1988 (s), 1923 (vs) cm^{-1}; also 2960 (vs), 2929 (m), 2862 (m), 1329 (s), 1255 (vs), 1031 (m), 811 (s), 487 (s) cm^{-1}. Satisfactory combustion analysis was not obtained after repeated attempts.

4.14. Synthesis of HRh(CNAr^{Dipp2})$_3$ (10)

To a solution of K[Rh(CNAr^{Dipp2})$_3$] (K[**3**]; 0.019 g, 0.014 mmol, 1 equiv) in 3 mL of C_6H_6, benzoic acid (0.0017 g, 0.014 mmol, 1 equiv) in an additional 1 mL of C_6H_6 was added dropwise. The reaction was let stir for 15 min before being filtered through a fiberglass syringe filter and dried in vacuo to yield an orange solid. Yield: 0.015 g, 0.011 mmol, 80%. X-ray quality crystals were grown by dissolving the solid in 2 mL of a *n*-pentane/benzene (20:1) solution and placing it at −32 ℃ for 3 days. ^{1}H NMR (499.8.9 MHz, C_6D_6, 20 ℃): δ = 7.35 (t, 4H, *J* = 8 Hz, *p*-Dipp), 7.30 (t, 2H, *J* = 8 Hz, *p*-Dipp), 7.22 (d, 8H, *J* = 8 Hz, *m*-Dipp), 7.17 (d, 4H, *J* = 8 Hz, *m*-Dipp), 6.94 (d, 2H, *J* = 8 Hz, *m*-Ar), 6.93 (dd, 2H, *J* = 8 Hz, *p*-Ar), 6.88 (d, 4H, *J* = 8 Hz, *m*-Ar), 6.80 (t, 1H, *J* = 8 Hz, *p*-Ar), 2.72 (septet, 8H, *J* = 7 Hz, C*H*(CH$_3$)$_2$), 2.60 (septet, 4H, *J* = 7 Hz, CH(C*H*$_3$)$_2$), 1.19 (d, 24H, *J* = 7 Hz, CH(C*H*$_3$)$_2$), 1.18 (d, 24H, *J* = 7 Hz, CH(C*H*$_3$)$_2$), 1.15 (d, 12H, *J* = 7 Hz, CH(C*H*$_3$)$_2$), 0.93 (d, 12H, *J* = 7 Hz, CH(C*H*$_3$)$_2$), −7.61 (d, 1H, *J* = 15.4 Hz, Rh*H*) ppm. ^{13}C{^{1}H} NMR (125.8 MHz, C_6D_6, 20 ℃): δ = 169.5 (*C*NR), 168.9 (*C*NR), 147.0, 146.9, 137.7, 135.9, 135.9, 130.6, 130.4, 130.1,129.7, 129.1, 128.6 127.3, 127.6, 126.2, 123.5, 123.3, 31.5, 31.1, 25.0, 24.8, 24.6, 24.5, 24.2 ppm. FTIR (KBr windows, C_6D_6, 20 ℃) υ(C≡N) = 2075 (m, sh), 2036 (vs), 2001 (s) cm^{-1}; also 3062 (w), 3023 (w), 2962 (s), 2927 (m), 2865 (m), 1577 (w), 1508 (w), 1457 (m), 1415 (m), 1384 (w), 1361 (w), 1334 (w), 1329 (w), 1253 (w), 1176 (w), 1056 (w), 813 (vs), 794 (w), 759 (s) cm^{-1}. Anal. Calcd. for $C_{93}H_{112}N_3Rh$: C, 81.25; H, 8.21; N, 3.06. Found: C, 81.30; H, 8.31; N, 3.13.

4.15. Synthesis of HIr(CNAr^{Dipp2})$_3$ (11)

To a solution of K[Ir(CNAr^{Dipp2})$_3$] (K[**4**]; 0.020 g, 0.013 mmol, 1 equiv) in 3 mL of C_6H_6, benzoic acid (0.0015 g, 0.013 mmol, 1 equiv) in an additional 1 mL of C_6H_6 was added dropwise. The reaction was let stir for 20 min before being filtered through a fiberglass syringe filter and dried in vacuo yielding a dark red solid. Yield: 0.015 g, 0.010 mmol, 77%. X-ray quality crystals were grown by dissolving the solid in 2 mL of a *n*-pentane/benzene (20:1) solution and placing it at −32 ℃ for 3 days. ^{1}H NMR (499.8.9 MHz, C_6D_6, 20 °C): δ = 7.33 (t, 4H, *J* = 8 Hz, *p*-Dipp), 7.29 (t, 2H, *J* = 8 Hz, *p*-Dipp), 7.20 (d, 8H, *J* = 8 Hz, *m*-Dipp), 7.17 (d, 4H, *J* = 8 Hz, *m*-Dipp), 6.89 (dd, 2H, *J* = 8 Hz, *m*-Ar), 6.89 (dd, 2H, *J* = 8 Hz, *p*-Ar), 6.93 (d, 4H, *J* = 8 Hz, *m*-Ar), 6.81 (t, 1H, *J* = 8 Hz, *p*-Ar), 2.72 (septet, 8H, *J* = 7 Hz, C*H*(CH$_3$)$_2$), 2.60 (septet, 4H, *J* = 7 Hz, CH(C*H*$_3$)$_2$), 1.18 (d, 24H, *J* = 7 Hz, CH(C*H*$_3$)$_2$), 1.16 (d, 24H, *J* = 7 Hz, CH(C*H*$_3$)$_2$), 1.13 (d, 12H, *J* = 7 Hz, CH(C*H*$_3$)$_2$), 0.90 (d, 12H, *J* = 7 Hz, CH(C*H*$_3$)$_2$), –2.45 (s, 1H, Ir*H*) ppm. ^{13}C{^{1}H} NMR (125.8 MHz, C_6D_6, 20 ℃): δ = 168.1 (*C*NR), 163.5 (*C*NR), 147.0, 146.9, 137.8, 137.2, 136.0, 135.9, 131.2, 130.6, 130.1, 130.8, 130.5 129.2, 129.0, 128.6 127.3, 127.6, 126.2, 124.9, 123.5, 123.4, 123.0, 31.2, 31.1, 25.1, 24.8, 24.7, 24.7, 24.6 ppm. FTIR (KBr windows, C_6D_6, 20 ℃) υ(C≡N) = 2082 (m, sh), 2032 (vs), 2005 (vs) cm^{-1}; also 2962 (s), 2927 (m), 2862 (m), 1735 (w), 1693 (w), 1577 (w), 1457 (m), 1446 (m), 1415 (m), 1384 (w), 1361 (w), 1334 (w), 1056 (w), 809 (m), 759 (s), 713 (w) cm^{-1}. Anal. Calcd. for $C_{93}H_{112}N_3Ir$: C, 76.29; H, 7.71; N, 2.87. Found: C, 75.23; H, 7.91; N, 2.10.

4.16. Synthesis of K[trans-Rh(SiMe$_3$)$_2$(CNAr^{Dipp2})$_2$] (12)

To a stirring solution of K[Rh(CNAr^{Dipp2})$_3$] (K[**3**]; 0.045 g, 0.032 mmol, 1 equiv) in 4 mL of an Et$_2$O/*n*-pentane (3:1) solution, hexamethyldisilane (65 μL, 0.319 mmol, 10 equiv) was added via micro-syringe. The reaction was let stir for 3 h after which X-ray quality crystals had formed at the edge of the meniscus which were used for single crystal X-ray diffraction analysis. The remaining solid and solution was cooled in a liquid-nitrogen cold well until a dark precipitate formed. It was then filtered over celite and washed with chilled *n*-pentane (3 × 2 mL), before being washed through with 10 mL of benzene. The benzene solution was lyophilized to yield a brown solid. Yield: 0.035 g, 0.031 mmol, 95%. ^{1}H NMR (499.8.9 MHz, C_6D_6, 20 ℃): δ = 7.17 (t, 4H, *J* = 8 Hz, *p*-Dipp), 7.13 (d, 8H, *J* = 8 Hz, *m*-Dipp), 7.04 (d, 4H, *J* = 8 Hz, *m*-Ar), 6.88 (t, 2H, *J* = 8 Hz, *p*-Ar), 2.96 (septet, 12H, *J* = 7 Hz, C*H*(CH$_3$)$_2$), 1.37 (d, 24H, *J* = 7 Hz, CH(C*H*$_3$)$_2$), 1.04 (d, 24H, *J* = 7 Hz, CH(C*H*$_3$)$_2$), 0.21 (s, 18H, Si(C*H*$_3$)$_3$) ppm. ^{13}C{^{1}H} NMR (125.8 MHz, THF-d_8, 20 ℃): δ = 197.7 (d, J_{RhC} = 63 Hz, *C*NR), 148.5, 138.4, 131.7, 131.3, 128.6, 127.5, 123.1, 122.7, 31.1, 30.9, 30.3, 25.9, 24.0, 8.6 ppm. FTIR (KBr windows, C_6D_6, 20 ℃) υ(C≡N) = 1974 (sh), 1901 (vs) cm^{-1}; also 2962 (s), 2927 (m), 2870 (m), 1574 (m), 1458 (m), 1408 (s), 1385 (w), 1361 (w), 1331 (w), 1223 (w), 810 (s), 707 (w) cm^{-1}. Anal. Calcd. for $C_{93}H_{111}N_3RhTl$: C, 71.92; H, 8.17; N, 2.47. Found: C, 71.14; H, 7.89; N, 2.35.

4.17. Computational details

Density Functional Theory (DFT) calculations were performed with ORCA 4.0.0 program suite [58]. Geometry optimizations, were performed using the B3LYP functional [59–61] in conjunction with the 6–31g(d) basis setfor H, C, O and N atoms [62], and the LANL2DZ basis set plus f-type polarization functions for the rhodium atoms [63]. Atomic coordinates obtained by single-crystal X-ray diffraction analysis on [K(crypt)][3] were used as the starting point for optimizations on the truncated model, [Rh(CNAr^{Ph2})$_3$]$^-$. Optimizations on [Rh(CO)$_3$]$^-$ used an idealized D_{3h}-symmetric complex as a starting point. *ChemCraft 1.8* was used for visualization of geometry optimized structures and molecular orbitals (MO) [64]. Full details for computational input and results can be found in the Supporting Informtion.

4.18. Crystallographic structure determinations

Single-crystal X-ray structure determinations were carried out at low temperature on a Bruker *P*4, Platform or Kappa Diffractometer equipped with a Mo or Cu radiation source. Data were acquired with Bruker APEX II, Photon II or Dextris Eiger 1 M detectors. All structures were solved via direct methods with SHELXS [65,66] and refined by full-matrix least-squares procedures using SHELXL [65,66] within the Olex2 software package [67]. Full details for crystallographic data collection and refinement can be found in the Supporting Information.

5. Dedication

Dedicated to Professor Arnold L. Rheingold, a tremendous mentor and great friend, on the occasion of his 80th birthday.

Declaration of Competing Interest

The authors declare that they have no known competing financial

interests or personal relationships that could have appeared to influence the work reported in this paper.

Data availability

Data will be made available on request.

Acknowledgements

We are grateful to the U.S. National Science Foundation for support of this work (CHE-1802646) and U.C. San Diego for a Roger Y. Tsien Fellowship to M.L.N.

Appendix A. Supplementary data

CCDC **2077996–2077810** contain the supplementary crystallographic data for all complexes. These data can be obtained free of charge via http://www.ccdc.cam.ac.uk/conts/retrieving.html, or from the Cambridge Crystallographic Data Centre, 12 Union Road, Cambridge CB2 1EZ, UK; fax: (+44) 1223-336-033; or e-mail: deposit@ccdc.cam.ac.uk. Supplementary data (computational and crystallographic) to this article can be found online at https://doi.org/10.1016/j.poly.2023.116565.

References

[1] H. Behrens, Four decades of metal carbonyl chemistry in liquid ammonia: aspects and prospects, Adv. Organomet. Chem. 18 (1980) 1–53.
[2] J.E. Ellis, Highly reduced metal carbonyl anions: synthesis, characterization, and chemical properties, Adv. Organomet. Chem. 31 (1990) 1–51.
[3] J.E. Ellis, Metal Carbonyl Anions: from $[Fe(CO)_4]^{2-}$ to $[Hf(CO)6]^{2-}$ and Beyond, Organometallics 22 (2003) 3322–3338.
[4] J.E. Ellis, Adventures with Substances Containing Metals in Negative Oxidation States, Inorg. Chem. 45 (2006) 3167–3186.
[5] L. Weber, Homoleptic Isocyanide Metalates, Angew. Chem. Int. Ed. 37 (1998) 1515–1517.
[6] J.P. Collman, Disodium tetracarbonylferrate: A Transition Metal Analog of a Grignard Reagent, Acc. Chem. Res. 8 (1975) 342–347.
[7] J.E. Ellis, The Chatt Reaction: Conventional Routes to Homoleptic Arenemetalates of d-Block Elements, Dalton Trans. 48 (2019) 9538–9563.
[8] J.E. Ellis, P.T. Barger, M.L. Winzenburg, Derivatives of Tricarbonylmetallates(-III) of Cobalt, Rhodium, and Iridium, J. Chem. Soc., Chem. Commun. (1977) 686–687.
[9] J.E. Ellis, C.P. Parnell, G.P. Hagen, Highly reduced organometallics. 3. Tetrasodium tetracarbonylmetalates(4-) of chromium, molybdenum, and tungsten, $Na_4M(CO)_4$, J. Am. Chem. Soc. 100 (1978) 3605–3607.
[10] J. M. Allen, W. W. Brennessel, C. E. Buss, J. E. Ellis, M. E. Minyaev, M. Pink, G. F. Warnock, M. L. Winzenburg, V. G. Young, Synthesis, Isolation, and Characterization of Trisodium Tricarbonyliridate (3−), Na3[Ir(CO)3]. Initial Studies on Its Derivative Chemistry and Structural Characterizations of trans-$[Ir(CO)_3(EPh_3)_2]^-$, E = Ge, Sn, and trans-$[Co(CO)_3(SnPh3)2]^-$, *Inorg. Chem.* **2001**, *40*, 5279-5284.
[11] J.T. Moore, C.C. Lu, Catalytic Hydrogenolysis of Aryl C-F Bonds Using a Bimetallic Rhodium-Indium Complex, J. Am. Chem. Soc. 142 (2020) 11641–11646.
[12] P. Wang, J. Cheng, D. Wang, C. Yang, X. Leng, L. Deng, Cobalt(−I)- and Rhodium (−I)-Mediated Dearylation of *N*-Aryl *N*–Heterocyclic Carbene Ligands, Organometallics 39 (2020) 2871–2877.
[13] V. Varela-Izquierdo, J.A. Ljpez, B. de Bruin, C. Tejel, M.a., Ciriano *T*hree-Coordinate Rhodium Complexes in Low Oxidation States, Chem. Eur. J. 26 (2020) 3270–3274.
[14] B.J. Fox, Q.Y. Sun, A.G. Dipasquale, A.R. Fox, A.L. Rheingold, J.S. Figueroa, Solution behavior and structural properties of Cu(I) complexes featuring m-terphenyl isocyanides, Inorg. Chem. 47 (2008) 9010–9020.
[15] G.W. Margulieux, N. Weidemann, D.C. Lacy, C.E. Moore, A.L. Rheingold, J. S. Figueroa, Isocyano analogues of $[Co(CO)_4]^n$: a tetraisocyanide of cobalt isolated in three states of charge, J. Am. Chem. Soc. 132 (2010) 5033–5035.
[16] M.A. Stewart, C.E. Moore, T.B. Ditri, L.A. Labios, A.L. Rheingold, J.S. Figueroa, Electrophilic functionalization of well-behaved manganese monoanions supported by m-terphenyl isocyanides, Chem. Commun. 47 (2011) 406–408.
[17] A.E. Carpenter, G.W. Margulieux, M.D. Millard, C.E. Moore, N. Weidemann, A. L. Rheingold, J.S. Figueroa, Zwitterionic Stabilization of a Reactive Cobalt Tris-Isocyanide Monoanion by Cation Coordination, Angew. Chem. Int. Ed. 51 (2012) 9412–9416.
[18] C.C. Mokhtarzadeh, G.W. Margulieux, A.E. Carpenter, N. Weidemann, C.E. Moore, A.L. Rheingold, J.S. Figueroa, Synthesis and Protonation of an Encumbered Iron Tetraisocyanide Dianion, Inorg. Chem. 54 (2015) 5579–5587.
[19] A.E. Carpenter, C. Chan, A.L. Rheingold, J.S. Figueroa, A Well-Defined Isocyano Analogue of HCo(CO)4. 2: Relative Brønsted Acidity as a Function of Isocyanide Ligation, Organometallics 35 (2016) 2319–2326.
[20] C.C. Mokhtarzadeh, C.E. Moore, A.L. Rheingold, J.S. Figueroa, Terminal Iron Carbyne Complexes Derived from Arrested CO_2 Reductive Disproportionation, Angew. Chem. Int. Ed. 56 (2017) 10894–10899.
[21] T. Ditri, B. Fox, C. Moore, A. Rheingold, J. Figueroa, Effective Control of Ligation and Geometric Isomerism: Direct Comparison of Steric Properties Associated with Bis-mesityl and Bis-diisopropylphenyl m-Terphenyl Isocyanides, Inorg. Chem. 48 (2009) 8362–8375.
[22] L.A. Labios, M.D. Millard, A.L. Rheingold, J.S. Figueroa, Bond Activation, Substrate Addition and Catalysis by an Isolable Two-Coordinate Pd (0) Bis-Isocyanide Monomer, J. Am. Chem. Soc. 131 (2009) 11318–11319.
[23] A.E. Carpenter, C.C. Mokhtarzadeh, D.S. Ripatti, I. Havrylyuk, R. Kamezawa, C. E. Moore, A.L. Rheingold, J.S. Figueroa, Comparative Measure of the Electronic Influence of Highly Substituted Aryl Isocyanides, Inorg. Chem. 54 (2015) 2936–2944.
[24] C.C. Mokhtarzadeh, A.E. Carpenter, D.P. Spence, M. Melaimi, D.W. Agnew, N. Weidemann, C.E. Moore, A.L. Rheingold, J.S. Figueroa, Geometric and Electronic Structure Analysis of the Three-Membered Electron-Transfer Series $[(\mu\text{-}CNR)_2[CpCo]_2]^n$ (n = 0, 1–, 2−) and Its Relevance to the Classical Bridging-Carbonyl System, Organometallics 36 (2017) 2126–2140.
[25] M.Y. Darensbourg, Ion Pairing Effects on Transition Metal Carbonyl Anions, Prog. Inorg. Chem. 33 (1985) 221–274.
[26] A. Macchioni, Ion Pairing in Transition-Metal Organometallic Chemistry, Chem. Rev. 105 (2005) 2039–2074.
[27] M. Zhou, L. Andrews, Reactions of Laser-Ablated Co, Rh, and Ir with CO: Infrared Spectra and Density Functional Calculations of the Metal Carbonyl Molecules, Cations and Anions in Solid Neon, J. Phys. Chem. A 103 (1999) 7773–7784.
[28] M.V. Barybin, V.G. Young, J.E. Ellis, Syntheses and Structural Characterizations of the First 16-, 17-, and 18-Electron Homoleptic Isocyanide Complexes of Vanadium: Hexakis(2,6-dimethyl- phenyl isocyanide)vanadium(I, 0, −I), J. Am. Chem. Soc. 120 (1998) 429–430.
[29] M.V. Barybin, W.W. Brennessel, B.E. Kucera, M.E. Minyaev, V.J. Sussman, V. G. Young, J.E. Ellis, Homoleptic Isocyanidemetalates of 4d- and 5d-Transition Metals: $[Nb(CNXyl)6]^-$, $[Ta(CNXyl)_6]^-$, and Derivatives Thereof, J. Am. Chem. Soc. 129 (2007) 1141–1150.
[30] W.W. Brennessel, J.E. Ellis, $[Fe(CNXyl)_4]^{2-}$: An Isolable and Structurally Characterized Homoleptic Isocyanidemetalate Dianion *Angew*, Chem. Int. Ed. 46 (2007) 598–600.
[31] B.M. Emerich, C.E. Moore, B.J. Fox, A.L. Rheingold, J.S. Figueroa, Protecting-Group-Free Access to a Three-Coordinate Nickel(0) Tris-isocyanide, Organometallics 30 (2011) 2598–2608.
[32] B.J. Fox, M.D. Millard, A.G. DiPasquale, A.L. Rheingold, J.S. Figueroa, Thallium(I) as a Coordination Site Protection Agent: Preparation of an Isolable Zero-Valent Nickel Tris-Isocyanide, Angew. Chem. Int. Ed. 48 (2009) 3473–3477.
[33] H.B. Gray, C.J. Ballhausen, A Molecular Orbital Theory for Square Planar Metal Complexes, J. Am. Chem. Soc. 85 (1963) 260–265.
[34] V. Albano, P.L. Bellon, V. Scatturin, Zerovalent metal complexes: crystal and molecular structure of $[Pt(PPh_3)_3]$, Chem. Commun. 507–507 (1966).
[35] C. Tejel, L. Asensio, M.P. del Río, B. de Bruin, J.A. López, M.A. Ciriano, Developing Synthetic Approaches with Non-Innocent Metalloligands: Easy Access to IrI/Pd0 and IrI/Pd0/IrI Cores, Angew. Chem. Int. Ed. 50 (2011) 8839–8843.
[36] J.C. Applegate, M.K. Okeowo, N.R. Erickson, B.M. Neal, C.L. Berrie, N. N. Gerasimchuk, M.V. Barybin, First π-linker featuring mercapto and isocyano anchoring groups within the same molecule: synthesis, heterobimetallic complexation and self-assembly on Au(111), Chem. Sci. 7 (2016) 1422–1429.
[37] M.J. Drance, J.D. Sears, A.M. Mrse, C.E. Moore, A.L. Rheingold, M.L. Neidig, J. S. Figueroa, Terminal Coordination of Diatomic Boron Monofluoride to Iron, Science 363 (2019) 1203–1205.
[38] S. Kim, F. Loose, P.J. Chirik, Beyond Ammonia: Nitrogen-Element Bond Forming Reactions with Coordinated Dinitrogen, Chem. Rev. 120 (2020) 5637–5681.
[39] M. Brookhart, M.L.H. Green, G. Parkin, Agostic interactions in transition metal compounds, Proc. Nat. Acad. Sci. USA 104 (2007) 6908–6914.
[40] T.-P. Lin, C.R. Wade, L.M. Pérez, F.P. Gabbaï, A Mercury→Antimony Interaction, Angew. Chem. Int. Ed. 49 (2010) 6357–6360.
[41] B.R. Barnett, C.E. Moore, P. Chandrasekaran, S. Sproules, A.L. Rheingold, S. DeBeer, J.S. Figueroa, Metal-Only Lewis Pairs Between Group 10 Metals and Tl (I) or Ag(I): Insights into the Electronic Consequences of Z-Type Ligand Binding, Chem. Sci. 6 (2015) 7169–7178.
[42] B.R. Barnett, J.S. Figueroa, Zero-valent Isocyanides of Nickel, Palladium and Platinum as Transition Metal s-type Lewis Bases *Chem*, Commun. 52 (2016) 13829–13839.
[43] M.V. Vollmer, J. Xie, C.C. Lu, Stable Dihydrogen Complexes of Cobalt(−I) Suggest an Inverse trans-Influence of Lewis Acidic Group 13 Metalloligands, J. Am. Chem. Soc. 139 (2017) 6570–6573.
[44] R.C. Cammarota, J. Xie, S.A. Burgess, M.V. Vollmer, K.D. Vogiatzis, J. Ye, J. C. Linehan, A.M. Appel, C. Hoffmann, X. Wang, V.G. Young, C.C. Lu, Thermodynamic and kinetic studies of H_2 and N_2 binding to bimetallic nickel-group 13 complexes and neutron structure of a Ni(η^2-H_2) adduct, Chem. Sci. 10 (2019) 7029–7042.
[45] D. You, F.P. Gabbaï, Tunable σ-Accepting, Z-Type Ligands for Organometallic Catalysis, Trends Chem. 1 (2019) 485–496.
[46] R.C. Cammarota, C.C. Lu, Tuning Nickel with Lewis Acidic Group 13 Metalloligands for Catalytic Olefin Hydrogenation, J. Am. Chem. Soc. 137 (2015) 12486–12489.
[47] M.D. Millard, C.E. Moore, A.L. Rheingold, J.S. Figueroa, Four-Coordinate Iridium (I) Monohydrides: Reversible Dinitrogen Binding, Bond Activations, and Deprotonations, J. Am. Chem. Soc. 132 (2010) 8921–8923.

[48] A.A. Danopoulos, D. Pugh, J.A. Wright, "Pincer" Pyridine–Dicarbene–Iridium Complexes: Facile C-H Activation and Unexpected η2-Imidazol-2-ylidene Coordination, Angew. Chem. Int. Ed. 47 (2008) 9765–9767.
[49] M. Feller, U. Gellrich, A. Anaby, Y. Diskin-Posner, D. Milstein, Reductive Cleavage of CO_2 by Metal–Ligand-Cooperation Mediated by an Iridium Pincer Complex, J. Am. Chem. Soc. 138 (2016) 6445–6454.
[50] Y. Pan, J.T. Mague, M.J. Fink, Organometallics 11 (1992) 3495–3497.
[51] M. Suginome, H. Oike, P.H. Shuff, Y. Ito, Double oxidative addition of the Si-Si and Si-Ge bonds onto isonitrile-platinum(0) complexes leading to the formation of tetrakis(organosilyl)- and bis(organogermyl)bis(organosilyl)platinum(IV) complexes, J. Organomet. Chem. 521 (1996) 405–408.
[52] M. Suginome, Y. Ito, Activation of silicon–silicon σ bonds by transition-metal complexes: synthesis and catalysis of new organosilyl transition-metal complexes, J. Chem. Soc., Dalton Trans (1998) 1925–1934.
[53] A. Roscher, A. Bockholt, T. Braun, Towards a catalytic hydrogenolysis of silicon-silicon bonds: Formation of Si–H bonds from disilanes and H2 at platinum, Dalton Trans. 1378–1382 (2009).
[54] M.B. Ansell, D.E. Roberts, F.G.N. Cloke, O. Navarro, J. Spencer, Synthesis of an $[(NHC)_2Pd(SiMe_3)_2]$ Complex and Catalytic cis-Bis(silyl)ations of Alkynes with Unactivated Disilanes *Angew*, Chem. Int. Ed. 54 (2015) 5578–5582.
[55] W.L.F. Arnarego, C.L.L. Chai, Purification of Laboratory Chemicals, 5th ed., Elsevier, 2003.
[56] A.B. Pangborn, M.A. Giardello, R.H. Grubbs, R.K. Rosen, F.J. Timmers, Safe and Convenient Procedure for Solvent Purification, Organometallics 15 (1996) 1518–1520.
[57] G. R.; Fulmer, A. J. M. Miller, N. H. Sherden, H. E. Gottlieb, A. Nudelman, B. M. Stoltz, J. E. Bercaw, K. I. Goldberg, NMR Chemical Shifts of Trace Impurities: Common Laboratory Solvents, Organics, and Gases in Deuterated Solvents Relevant to the Organometallic Chemist. *Organometallics* **2010,** *29*, 2176-2179.
[58] F. Neese, The ORCA program system. *Wiley Interdisciplinary Reviews: Computational Molecular Science* **2011,** *2* (1), 73-78.
[59] A.D. Becke, Density functional calculations of molecular bond energies, J. Chem. Phys. 84 (1986) 4524–4529.
[60] A.D. Becke, Density-functional thermochemistry. III. The role of exact exchange, J. Chem. Phys. 98 (1993) 5648–5652.
[61] C. Lee, W. Yang, R.G. Parr, R. g.,, Development of the Colle-Salvetti correlation-energy formula into a functional of the electron density, Phys. Rev. B 37 (1988) 785–789.
[62] G.A. Petersson, A. Bennett, T.G. Tensfeldt, M.A. Al-Laham, W.A. Shirley, J. Mantzaris, A complete basis set model chemistry. I. The total energies of closed-shell atoms and hydrides of the first-row elements, J. Chem. Phys. 89 (4) (1988) 2193–2218.
[63] P.J. Hay, W.R. Wadt, Ab initio effective core potentials for molecular calculations. Potentials for K to Au including the outermost core orbitals, J. Chem. Phys. 82 (1) (1985) 299–310.
[64] D. A. Zhurko, G. A.; Zhurko, "ChemCraft 2014," www.chemcraftprog.com, 2014.
[65] G.M. Sheldrick, A short history of SHELX, Acta Crystallogr. A 64 (2008) 112–122.
[66] G.M. Sheldrick, Crystal structure refinement with SHELXL, Acta Crystallogr. C 71 (2015) 3–8.
[67] O.V. Dolomanov, L.J. Bourhis, R.J. Gildea, J.A.K. Howard, H. Puschmann, OLEX2: a complete structure solution, refinement and analysis program, J. Appl. Crystallogr. 42 (2009) 339–341.